Synthesis

General.

All synthetic procedures were performed under N_2 atomosphere. ^{1}H, ^{13}C, and ^{11}B NMR spectra were recorded on JEOL JNM-AL400 (Charts S1–S6, S9–S12, and S14–S19) and JNM-ECZ400 (Charts S7, S8 and S20) instruments at 400, 100, and 128 MHz, respectively. ^{13}C NMR spectra in Chart S13 was recorded at the Technical Support Office (Department of Synthetic Chemistry and Biological Chemistry, Graduate School of Engineering, Kyoto University) by a JNM-ECZ600R instrument at 150 MHz. Samples were analyzed in $CDCl_3$ and CD_2Cl_2. The ^{1}H and ^{13}C chemical shift values were expressed relative to Me_4Si as an internal standard in $CDCl_3$ and residual solvent peak as an internal stanrard in CD_2Cl_2. The ^{11}B chemical shift values were expressed relative to $BF_3{\cdot}Et_2O$ as an external standard. Analytical thin-layer chromatography (TLC) was performed with silica gel 60 Merck F254 plates. Column chromatography was performed with Wakogel® C-300 silica gel. High-resolution mass (HRMS) spectrometry was performed at the Technical Support Office (Department of Synthetic Chemistry and Biological Chemistry, Graduate School of Engineering, Kyoto University), and the HRMS spectra were obtained on a Thermo Fisher Scientific EXACTIVE spectrometer for atmospheric pressure chemical ionization (APCI) and SHIMADZU GCMS-QP2010SE spectrometer for electron ionization (EI).

Materials. Tetrahydrofuran (THF) was purchased and purified by passage through purification column under N_2 pressure. Decaborane(14), *N*,*N*-dimethylaniline, *n*-butyllithium (1.6 M in *n*-hexane), palladium(II) acetate, tri-*tert*-butylphosphonium tetrafluoroborate, cesium carbonate, dimethyl (1-diazo-2-oxopropyl)phosphonate, methanol (MeOH), chloroform ($CHCl_3$), *n*-hexane, ethyl acetate (AcOEt), toluene, acetonitrile (MeCN), and dimethylformamide (DMF) were obtained commercially and used without purification. 1-Bromo-2-(2-bromophenyl)-naphthalene was synthesized and characterized according to the literature.[1]

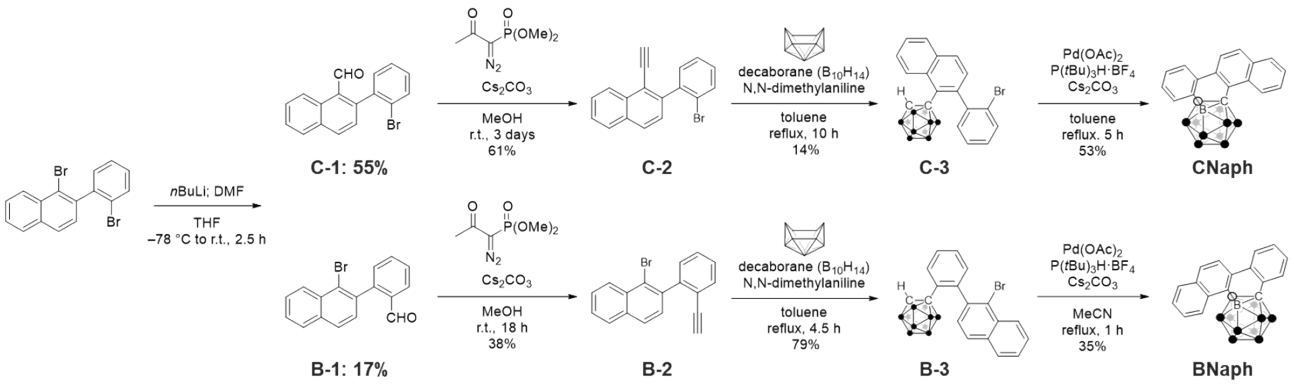

Scheme S1. Overall synthetic routes for **CNaph** and **BNaph**.

Synthesis of C-1 and B-1. *n*BuLi (1.9 mL, 1.6 M in hexane, 3.04 mmol) was added dropwise to the mixture of 1-bromo-2-(2-bromophenyl)-naphthalene (1.083 g, 2.98 mmol) and anhydrous THF (21 mL) at –78 °C. After addition, the mixture was stirred for 1 h at the same temperature, then DMF (0.517 g, 0.55 mL, 7.07 mmol) was added. The mixture was stirred at room temperature for 2.5 h. After addition of sat. NH_4Claq, the resulting mixture was extracted with AcOEt. The organic layer was washed with brine, dried with Na_2SO_4, filtrated and concentrated. The crude product was purified by silica gel column chromatography (*n*-hexane/toluene = 1/1 (v/v)) to give **C-1** as a dark yellow oil (0.508 g, 1.63 mmol, 55 %) and **B-1** as a yellow oil (0.155 g, 0.496 mmol, 17 %). **C-1**: ^{1}H NMR (400 MHz, $CDCl_3$): δ (ppm) 10.14 (1H, s), 9.33 (1H, d, *J* = 8.4 Hz), 8.11 (1H, d, *J* = 8.8 Hz), 7.95–7.93 (1H, m), 7.74–7.70 (2H, m), 7.64–7.60 (1H, m), 7.45–7.31 (4H, m). ^{13}C NMR (100 MHz, $CDCl_3$): δ (ppm) 193.8, 147.4, 139.7, 134.2, 133.5, 132.9, 131.9, 130.3, 129.9, 129.4, 128.5, 128.4, 128.1, 127.3, 127.1, 126.1, 123.6. HRMS (*p*-APCI): Calcd. for $C_{17}H_{12}BrO$ $[M+H]^+$ m/z 311.0066, found m/z 311.0071. **B-1**: ^{1}H NMR (400 MHz, $CDCl_3$): δ (ppm) 9.80 (1H, s), 8.38 (1H, dd, *J* = 8.4 Hz, 0.4 Hz), 8.08 (1H, dd, *J* = 8.0 Hz, 1.6 Hz), 7.93–7.89 (2H, m), 7.73–7.57 (4H, m), 7.43–7.38 (2H, m). ^{13}C NMR (100 MHz, $CDCl_3$): δ (ppm) 191.5, 145.7, 136.9, 133.9, 133.7, 133.6, 132.1, 13.8, 128.5, 128.3, 128.2, 128.2, 127.7, 127.7, 127.3, 127.2, 124.0. HRMS (*p*-APCI): Calcd. for $C_{17}H_{12}BrO$ $[M+H]^+$ m/z 311.0066, found m/z 311.0056.

Synthesis of C-2. Dimethyl(1-diazo-2-oxopropyl)phosphonate (0.122 g, 0.095 mL, 0.63 mmol) was added in one portion to the suspension of **C-1** (0.154 g, 0.49 mmol), Cs_2CO_3 (0.408 g, 1.25 mmol), and MeOH (10 mL). The mixture was stirred for 3 days at room temperature, then excess water was added. The resulting mixture was extracted with AcOEt, washed with brine, dried with Na_2SO_4, filtrated and concentrated. The crude product was purified by silica gel column chromatography

(elutent: *n*-hexane/AcOEt = 20/1 (v/v)) to give **C-2** as a colorless oil (0.094 g, 0.30 mmol, 61%). ^{1}H NMR (400 MHz, CD_2Cl_2): δ (ppm) 8.44 (1H, d, *J* = 8.4 Hz), 7.94–7.92 (2H), 7.74–7.72 (1H, m), 7.67–7.57 (2H, m), 7.44–7.39 (3H), m, 7.33–7.29 (1H, m), 3.45 (1H, s). ^{13}C NMR (100 MHz, CD_2Cl_2): δ (ppm) 143.5, 142.2, 133.9, 133.0, 132.8, 131.9, 129.7, 128.9, 128.6, 127.8, 127.7, 127.5, 127.1, 126.7, 123.5, 119.0, 86.2, 80.4. HRMS (*p*-APCI): Calcd. for $C_{18}H_{12}Br$ $[M+H]^+$ m/z 307.0117, found m/z 307.0121.

Synthesis of B-2. Dimethyl(1-diazo-2-oxopropyl)phosphonate (0.128 g, 0.10 mL, 0.67 mmol) was added in one portion to the suspension of **B-1** (0.183 g, 0.59 mmol), Cs_2CO_3 (0.351 g, 1.07 mmol), and MeOH (1.3 mL). The mixture was stirred for 18 h at room temperature, then excess water was added. The resulting mixture was extracted with AcOEt, washed with brine, dried with Na_2SO_4, filtrated and concentrated. The crude product was purified by silica gel column chromatography (elutent: n-hexane/AcOEt = 20/1 (v/v)) to give **B-2** as a yellow oil (0.069 g, 0.22 mmol, 38%). ^{1}H NMR (400 MHz, $CDCl_3$): δ (ppm) 8.40 (1H, d, *J* = 8.8 Hz), 7.90–7.87 (1H, m), 7.85 (1H, d, *J* = 8.4 Hz), 7.66–7.61 (2H, m), 7.58 (1H, ddd, *J* = 7.6 Hz, 7.4 Hz, 1.2 Hz), 7.47–7.33 (4H, m), 2.87 (1H, s). ^{13}C NMR (100 MHz, $CDCl_3$): δ (ppm) 143.2, 139.6, 133.9, 133.0, 132.4, 129.9, 128.5, 128.3, 128.2, 127.9, 127.7, 127.6, 127.2, 126.7, 123.3, 121.7, 82.2, 80.5. HRMS (p-EI): Calcd. for $C_{18}H_{11}Br$ $[M+H]^+$ m/z 306.0044, found m/z 306.0038.

Synthesis of C-3. The mixture of **C-2** (0.591 g, 1.92 mmol), decaborane(14) (0.253 g, 2.06 mmol), and *N*,*N*-dimethylaniline (0.43 mL, 3.4 mmol) were dissolved in toluene (19 mL) at room temperature. The mixture was refluxed for 10 h. After cooling to room temperature, the mixture was filtrated and evaporated. The crude product was purified by silica gel column chromatography (eluent: *n*-hexane), and the obtained solid was XXXecrystallized from MeOH/$CHCl_3$ at 60 °C to afford **C-3** as a colorless solid (115.5 mg, 0.272 mmol, 14%). ^{1}H NMR (400 MHz, CD_2Cl_2): δ (ppm) 9.31 (1H, d, *J* = 8.8 Hz), 7.90–7.86 (2H, m), 7.79 (1H, dd, *J* = 8.2 Hz, 1.6 Hz), 7.63–7.56 (2H, m), 7.46–7.33 (3H, m), 7.04 (1H, d, *J* = 8.4 Hz), 4.08 (1H, s), 3.91–1.12 (10H, br). ^{13}C NMR (100 MHz, CD_2Cl_2): δ (ppm) 143.2, 139.3, 135.0, 134.2, 132.0, 131.7, 131.2, 130.9, 130.8, 129.5, 128.1, 127.8, 126.9, 126.72, 126.66, 123.5, 77.6, 63.3. ^{11}B NMR (128 MHz, CD_2Cl_2): δ (ppm) –1.28 to –4.22 (2B), –8.93 to –14.72 (8B). HRMS (*n*-APCI): Calcd. for $C_{18}H_{21}B_{10}Br$ $[M]^-$ m/z 426.1815, found m/z 426.1821.

Synthesis of B-3. The mixture of **B-2** (1.474 g, 4.79 mmol), decaborane(14) (0.619 g, 5.06 mmol), and *N*,*N*-dimethylaniline (1.1 mL, 8.7 mmol) were dissolved in toluene (48 mL) at room temperature. The mixture was refluxed for 4.5 h. After cooling to room temperature, the mixture was filtrated and evaporated. The crude product was purified by silica gel column chromatography (eluent: *n*-hexane), and the obtained solid was recrystalized from MeOH/$CHCl_3$ at 65 °C to afford **B-3** as a colorless solid (1.607 g, 3.78 mmol, 79%). ^{1}H NMR (400 MHz, CD_2Cl_2): δ (ppm) 8.38–8.35 (1H, m), 7.97–7.95 (1H, m), 7.92 (1H, d, *J* = 8.4 Hz), 7.84–7.78 (1H, m), 7.72 (1H, ddd, *J* = 7.7 Hz, 7.6 Hz, 1.6 Hz), 7.66 (1H, ddd, *J* = 7.6 Hz, 7.5 Hz, 1.6 Hz), 7.49–7.41 (2H, m), 7.37 (1H, d, 8.0 Hz), 7.06–7.03 (1H, m), 3.41 (1H, s), 3.31–1.00 (10H, br). ^{13}C NMR (150 MHz, CD_2Cl_2): δ (ppm) 139.7, 139.2, 134.4, 133.3, 132.8, 132.7, 131.0, 129.4, 128.97, 128.91, 128.87, 128.2, 128.14, 128.13, 128.09, 124.9, 77.6, 58.5. ^{11}B NMR (128 MHz, CD_2Cl_2): δ (ppm) –3.34 to –4.42 (2B), –8.93 to –14.62 (8B). HRMS (*n*-APCI): Calcd. for $C_{18}H_{21}B_{10}BrCl$ $[M+Cl]^-$ m/z 461.1503, found m/z 461.1507.

Synthesis of CNaph. The mixture of **C-3** (13.9 mg, 0.033 mmol), $Pd(OAc)_2$ (0.9 mg, 0.0040 mmol), P(*t*Bu)$_3$H·BF_4 (1.6 mg, 0.0055 mmol), and Cs_2CO_3 (26.8 mg, 0.082 mmol) were dissolved in toluene (1.4 mL) at room temperature. The resulting mixture was refluxed for 5 h. After hydrolysis with water and extraction with AcOEt, the combined organic phase was washed with brine and dried over Na_2SO_4. After filtration, the solvent was evaporated. The residue was purified by column chromatography on a silica gel (eluent: *n*-hexane/AcOEt = 10/1 (v/v)). After evaporation of solvents, the desired product was isolated with recrystallization from *n*-hexane (75 °C) as a colorless solid (6.0 mg, 0.017 mmol, 53%). ^{1}H NMR (400 MHz, $CDCl_3$): δ (ppm) 9.47 (1H, d, *J* = 9.2 Hz), 8.35 (1H, d, *J* = 8.8 Hz), 8.19 (1H, d, *J* = 8.4 Hz), 8.08 (1H, dd, *J* = 7.6 Hz, 1.2 Hz), 8.03 (1H, d, 8.8 Hz), 7.88 (1H, dd, *J* = 8.2 Hz, 1.6 Hz), 7.67 (1H, ddd, *J* = 8.8 Hz, 7.9 Hz, 1.6 Hz), 7.62 (1H, ddd, *J* = 7.7 Hz, 7.6 Hz, 1.6 Hz), 7.56 (1H, dd, *J* = 7.6 Hz, 7.6 Hz), 7.53 (1H, dd, *J* = 7.2 Hz, 7.2 Hz), 3.19 (1H, s), 3.44–1.72 (9H, br). ^{13}C NMR (100 MHz, $CDCl_3$): δ (ppm) 135.5, 135.05, 135.04, 133.9, 132.6, 131.9, 130.4, 129.1, 128.9, 127.1, 126.9, 126.5, 126.2, 124.2, 124.1, 72.8, 61.8 (C_{aryl}–B_{cage} signal was not observed). ^{11}B NMR (128 MHz, $CDCl_3$): δ (ppm) –2.26 to –14.53 (10B). HRMS (*n*-APCI): Calcd. for $C_{18}H_{20}B_{10}$ $[M]^-$ m/z 346.2501, found m/z 346.2499.

Synthesis of BNaph. The mixture of **B-3** (0.426 g, 1.00 mmol), $Pd(OAc)_2$ (0.023 g, 0.10 mmol), P(*t*Bu)$_3$H·BF_4 (0.060 g, 0.21 mmol), and Cs_2CO_3 (0.672 g, 2.06 mmol) were dissolved in MeCN (40

mL) at room temperature. The resulting mixture was refluxed for 1 h. After hydrolysis with water and extraction with AcOEt, the combined organic phase was washed with brine and dried over Na_2SO_4. After filtration, the solvent was evaporated. The residue was purified by column chromatography on a silica gel (eluent: *n*-hexane). After evaporation of solvents, the desired product was isolated with recrystallization from MeOH/$CHCl_3$ (60 °C) as a colorless solid (0.121 g, 0.35 mmol, 35%). ^{1}H NMR (400 MHz, $CDCl_3$): δ (ppm) 9.40 (1H, d, J = 8.8 Hz), 8.29 (1H, d, J = 8.4 Hz), 8.25 (1H, d, J = 9.2 Hz), 8.00 (1H, d, 8.8 Hz), 7.91 (1H, dd, J = 8.0 Hz, 1.2 Hz), 7.88 (1H, dd, J = 8.0 Hz, 1.2 Hz), 7.66 (1H, ddd, J = 8.0 Hz, 7.8 Hz, 1.6 Hz), 7.61–7.56 (2H, m), 7.42 (1H, ddd, J = 7.8 Hz, 7.6 Hz, 1.2 Hz), 3.13 (1H, s), 3.81–1.33 (9H, br). ^{13}C NMR (100 MHz, $CDCl_3$): δ (ppm) 136.7, 134.6, 133.6, 133.1, 132.7, 131.4, 131.1, 129.0, 128.9, 128.5, 128.3, 127.2, 127.0, 126.7, 122.5, 74.1, 59.9 (C_{aryl}–B_{cage} signal was not observed). ^{11}B NMR (128 MHz, $CDCl_3$): δ (ppm) –2.62 (1B, d, J = 150.0 Hz), –5.23 (1B, d, J = 148.6 Hz), –7.58 to –14.59 (8B). HRMS (*n*-APCI): Calcd. for $C_{18}H_{20}B_{10}$ $[M]^-$ m/z 346.2501, found m/z 346.2507.

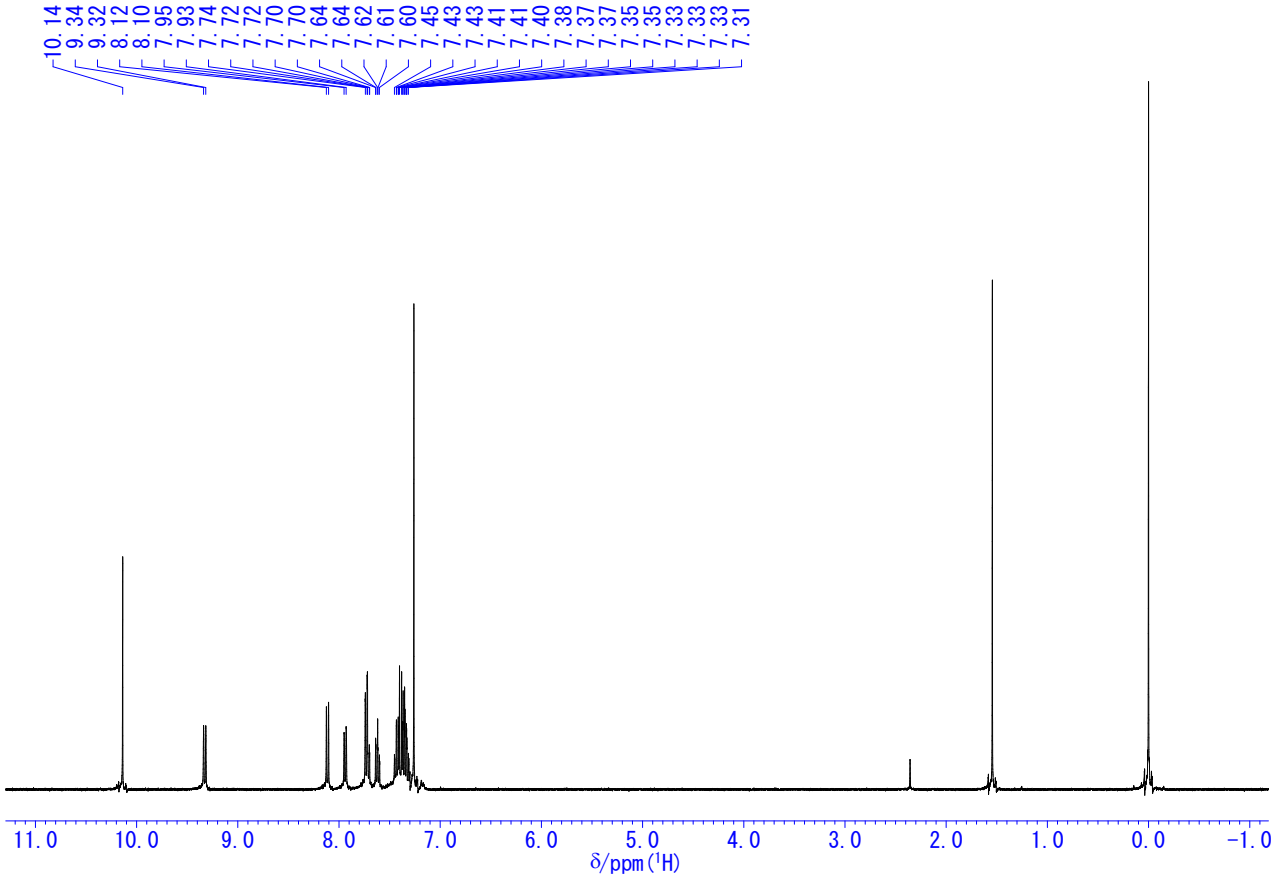

Chart S1. ^{1}H NMR spectrum of **C-1** in $CDCl_3$.

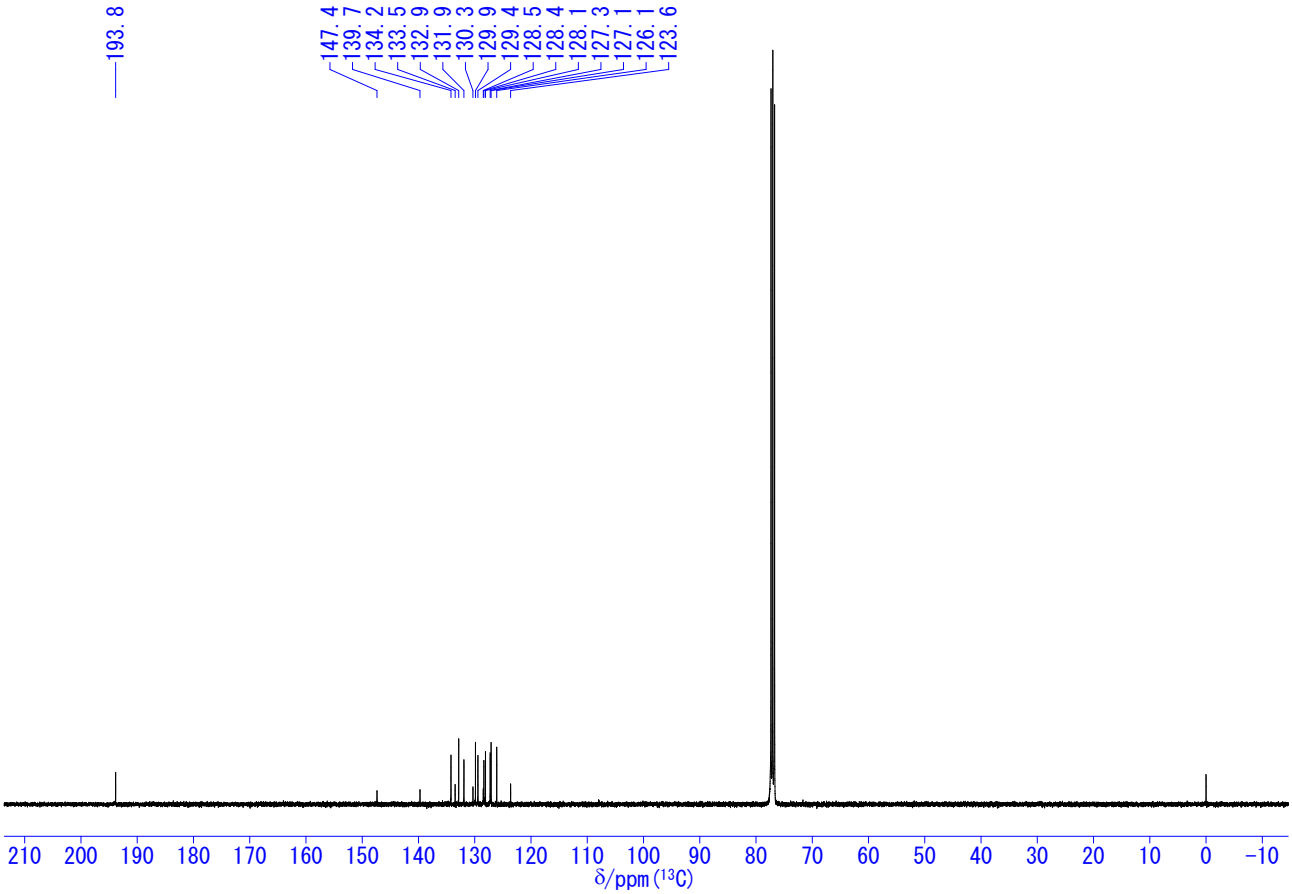

Chart S2. ^{13}C NMR spectrum of **C-1** in $CDCl_3$.

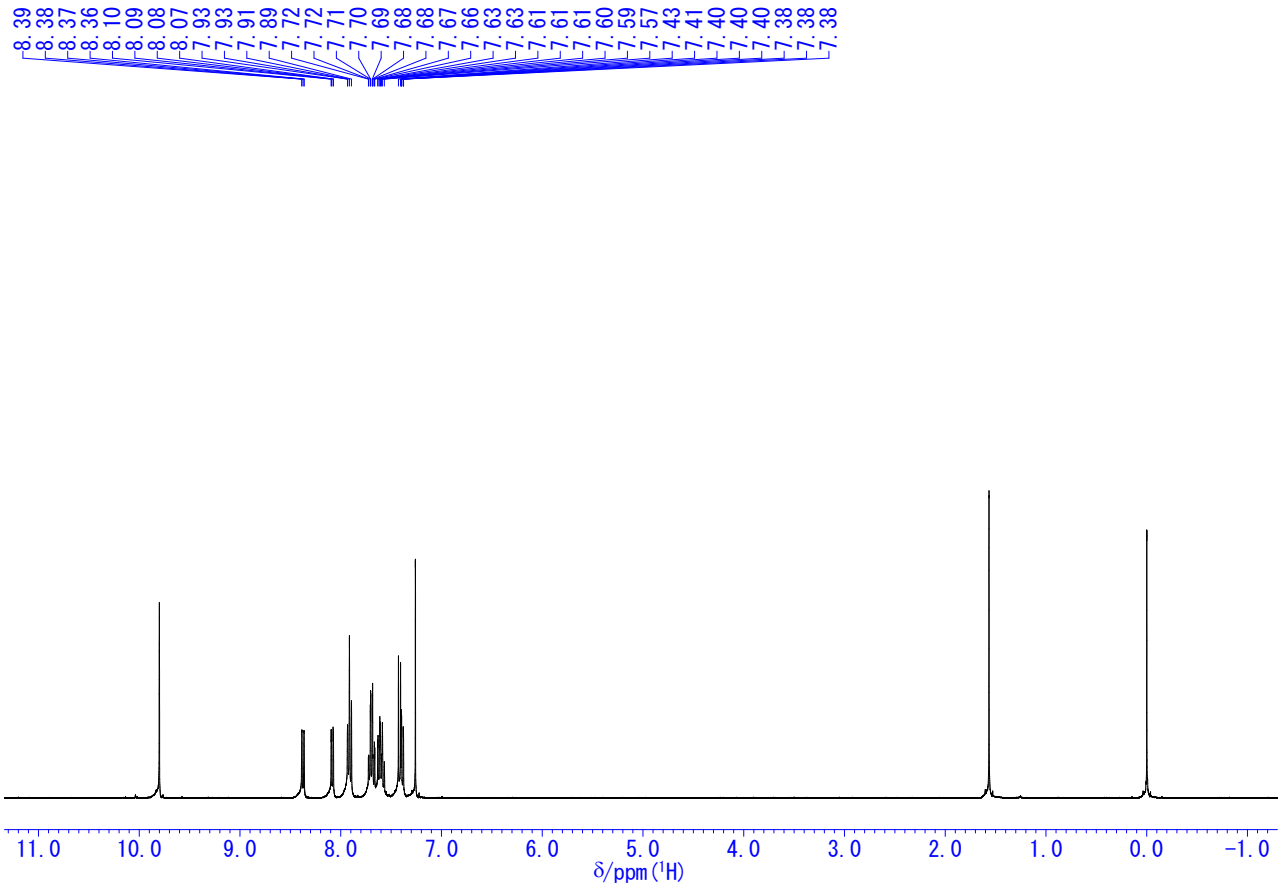

Chart S3. ^{1}H NMR spectrum of **B-1** in $CDCl_3$.

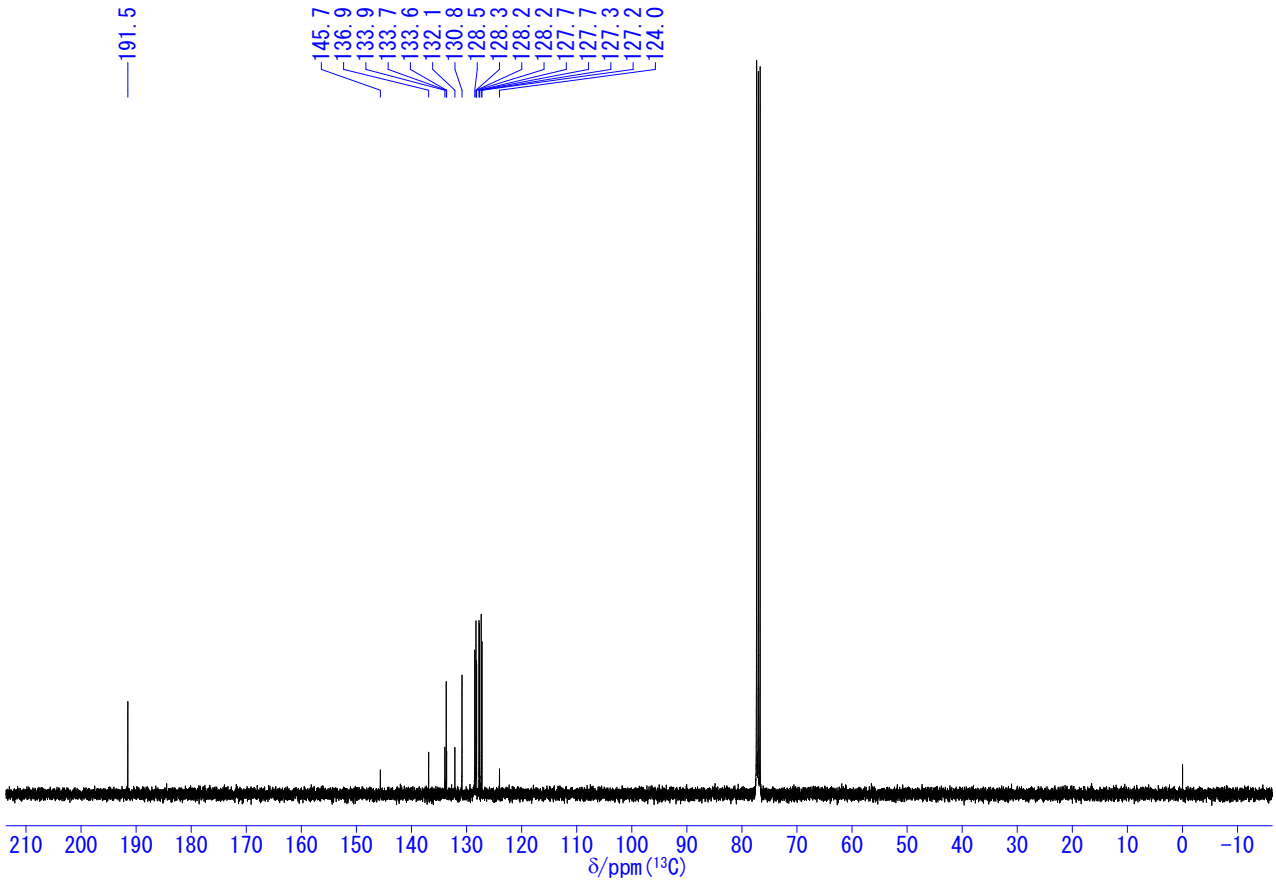

Chart S4. ^{13}C NMR spectrum of **B-1** in $CDCl_3$.

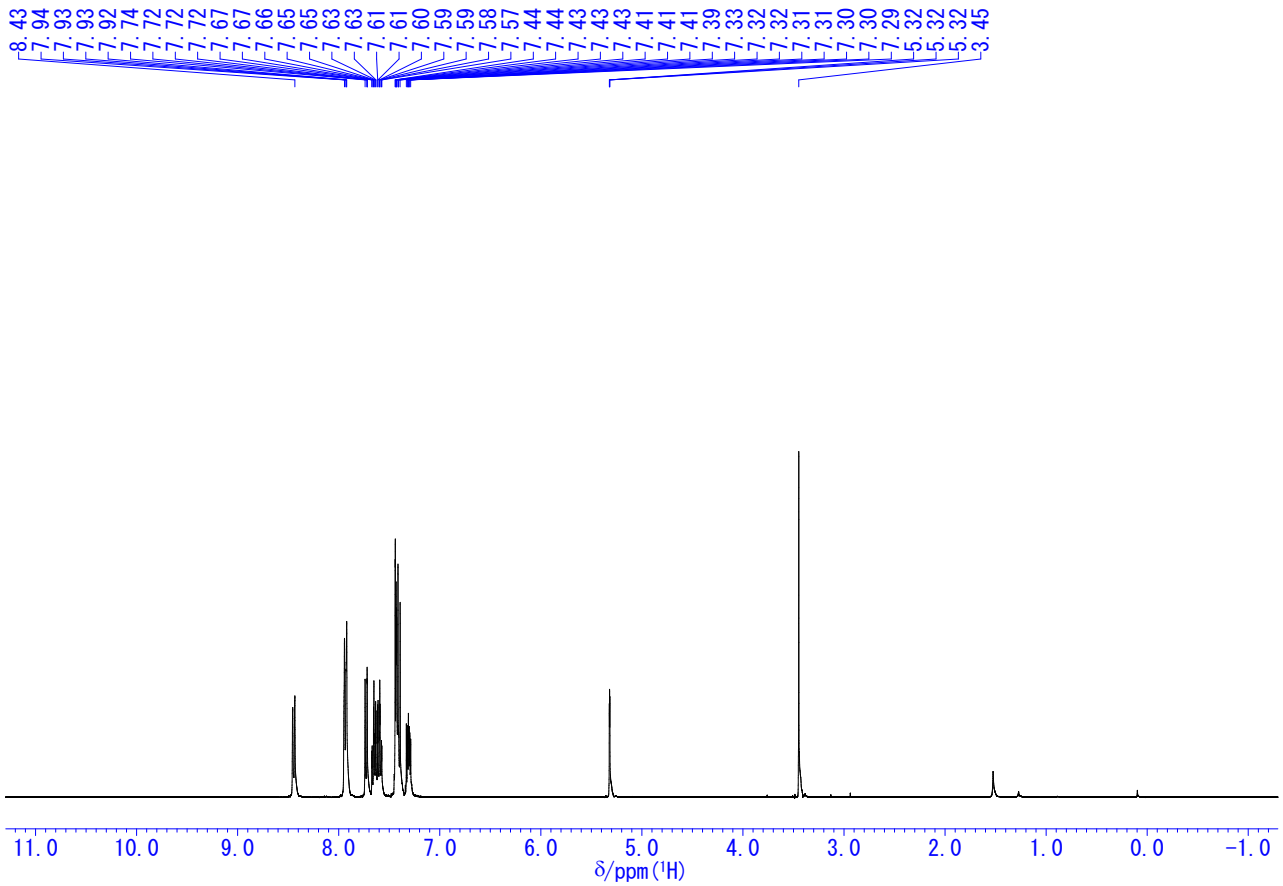

Chart S5. ^{1}H NMR spectrum of **C-2** in CD_2Cl_2.

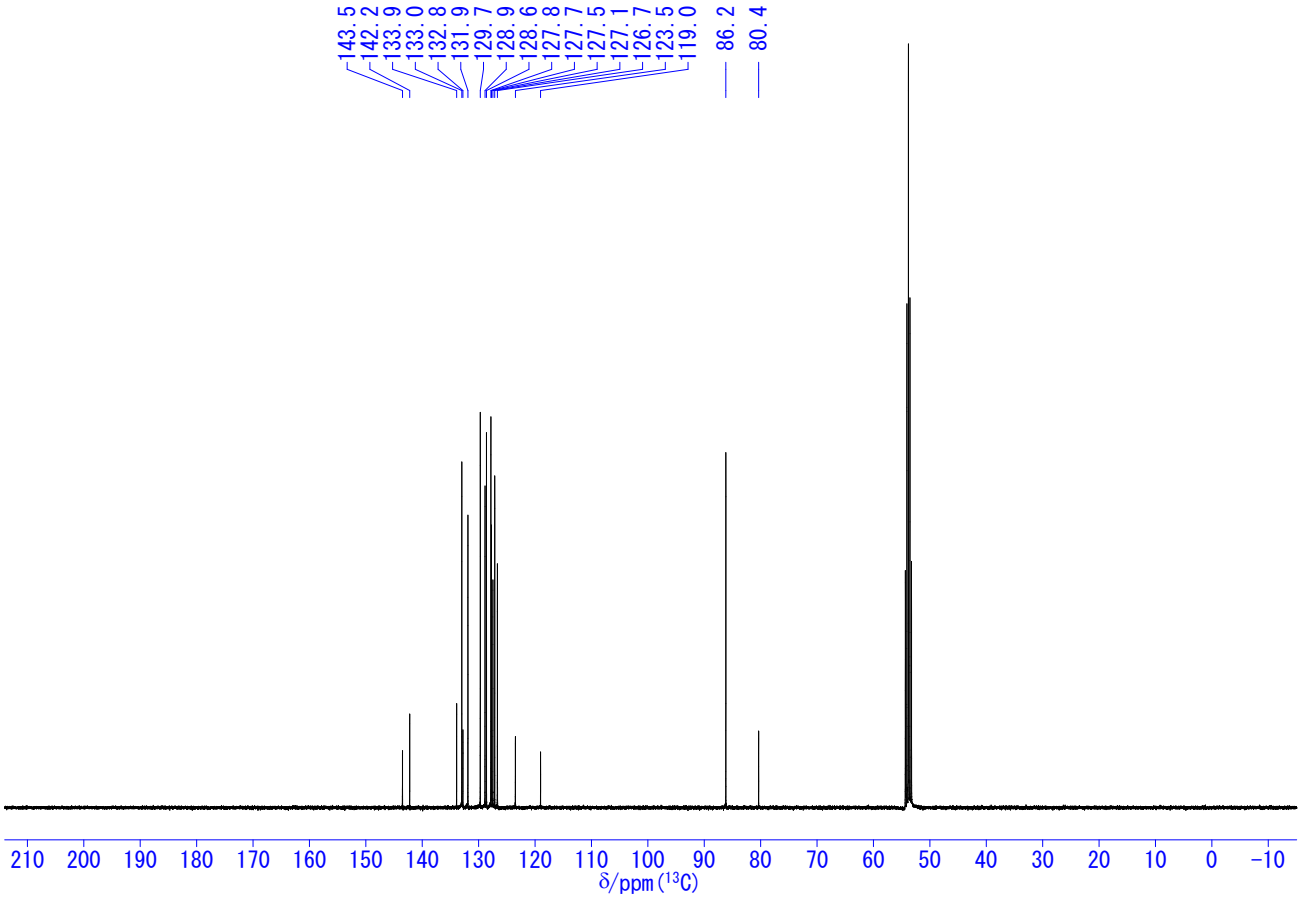

Chart S6. ^{13}C NMR spectrum of **C-2** in CD_2Cl_2.

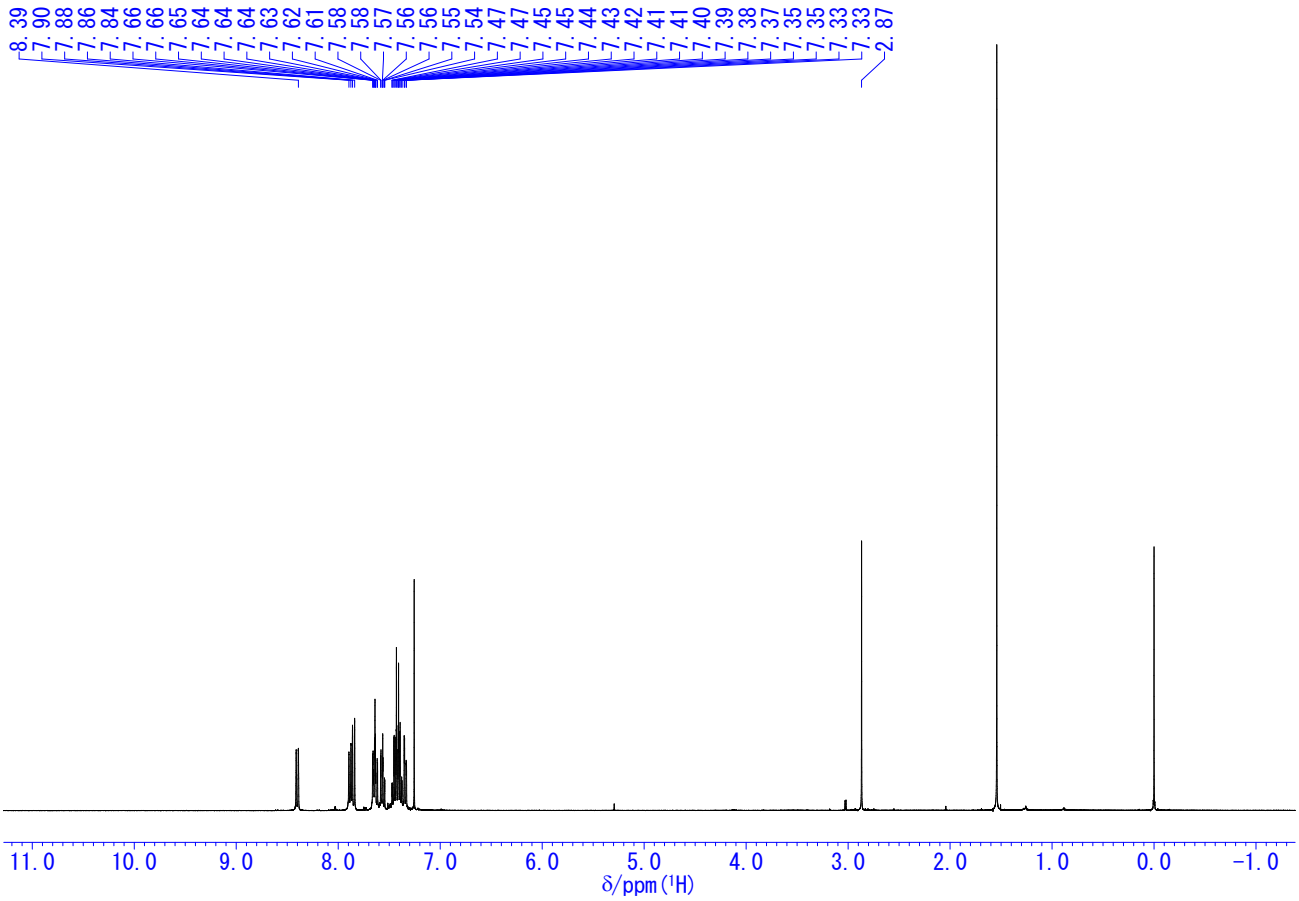

Chart S7. ^{1}H NMR spectrum of **B-2** in $CDCl_3$.

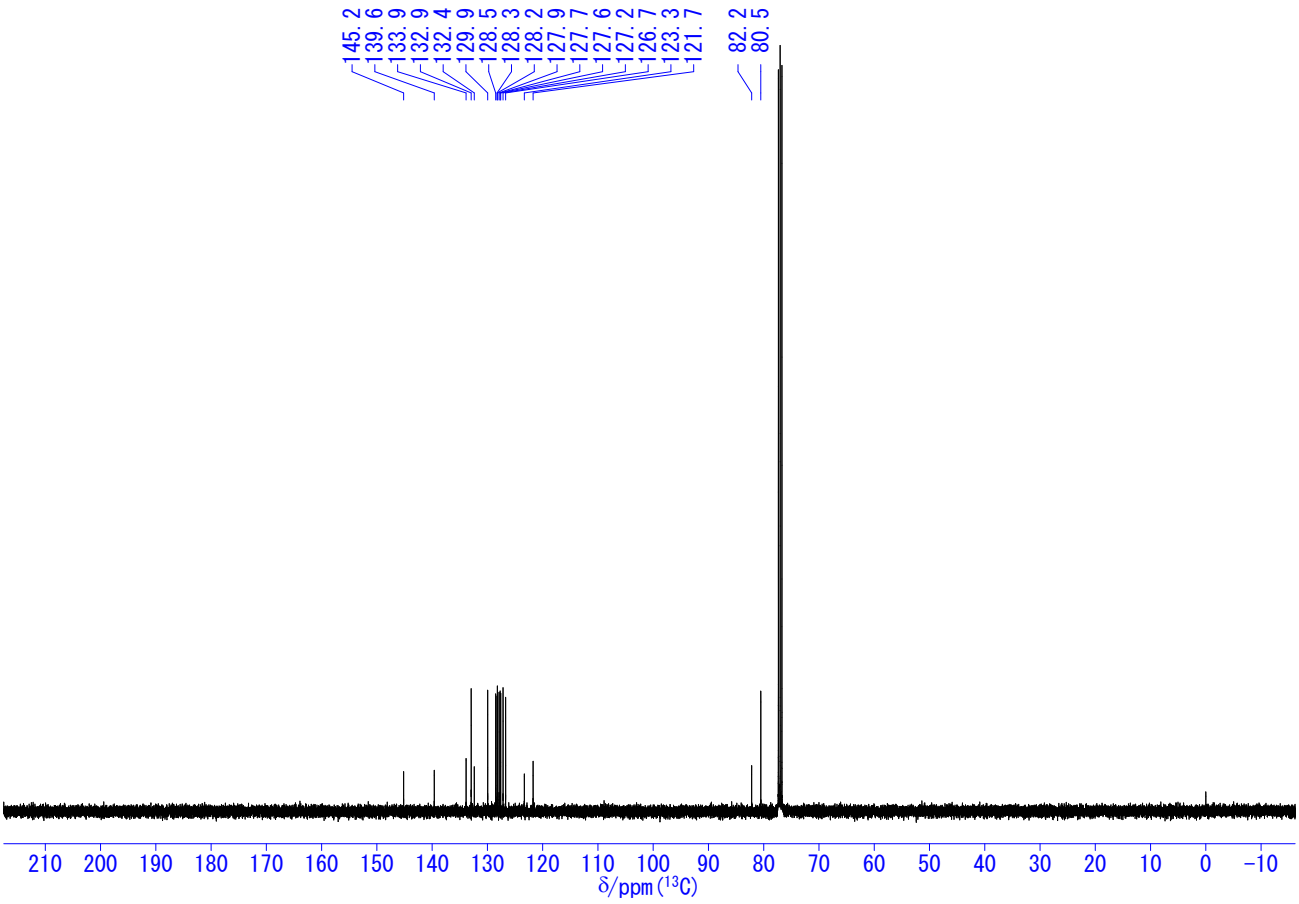

Chart S8. ^{13}C NMR spectrum of **B-2** in $CDCl_3$.

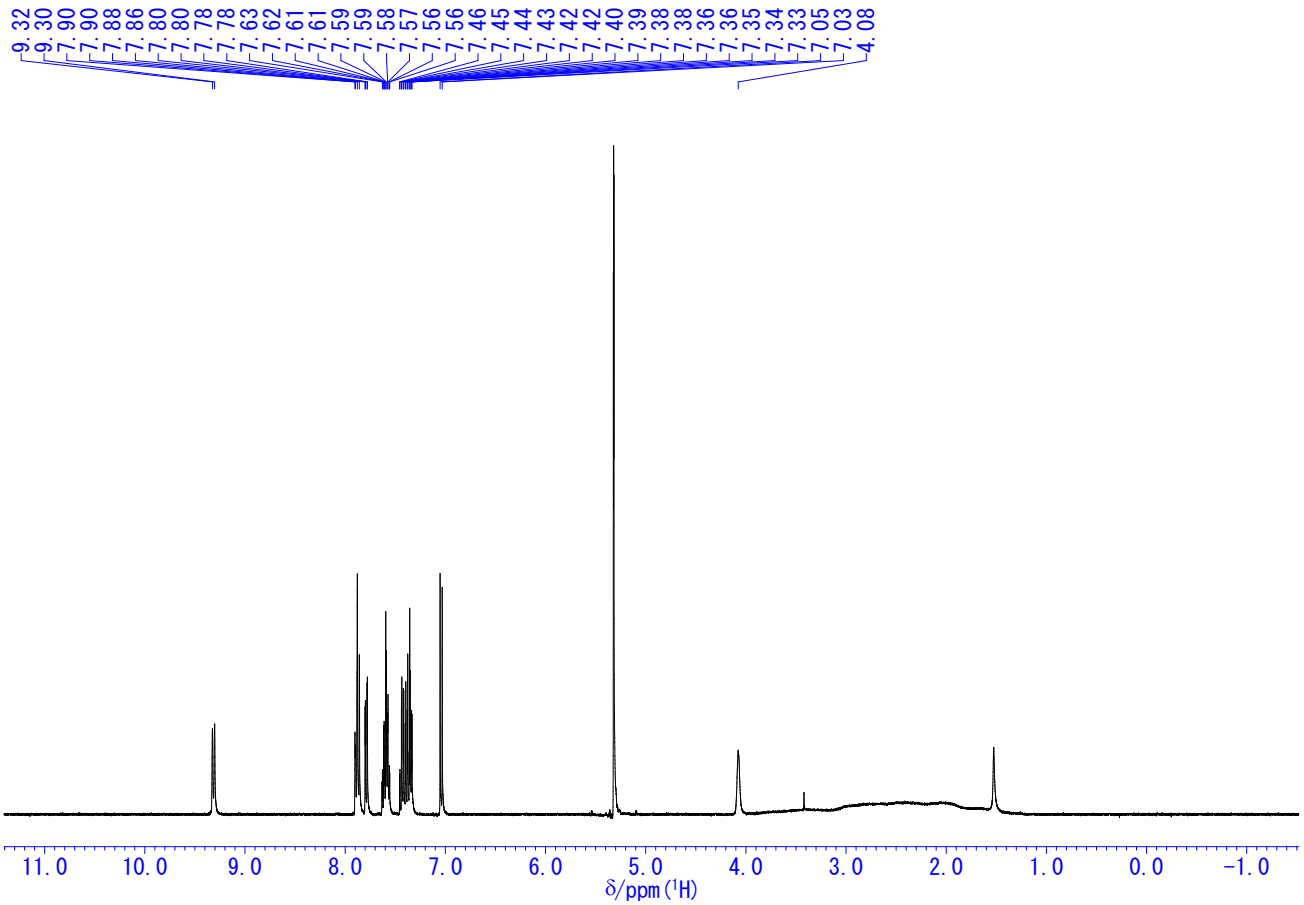

Chart S9. ^{1}H NMR spectrum of **C-3** in CD_2Cl_2.

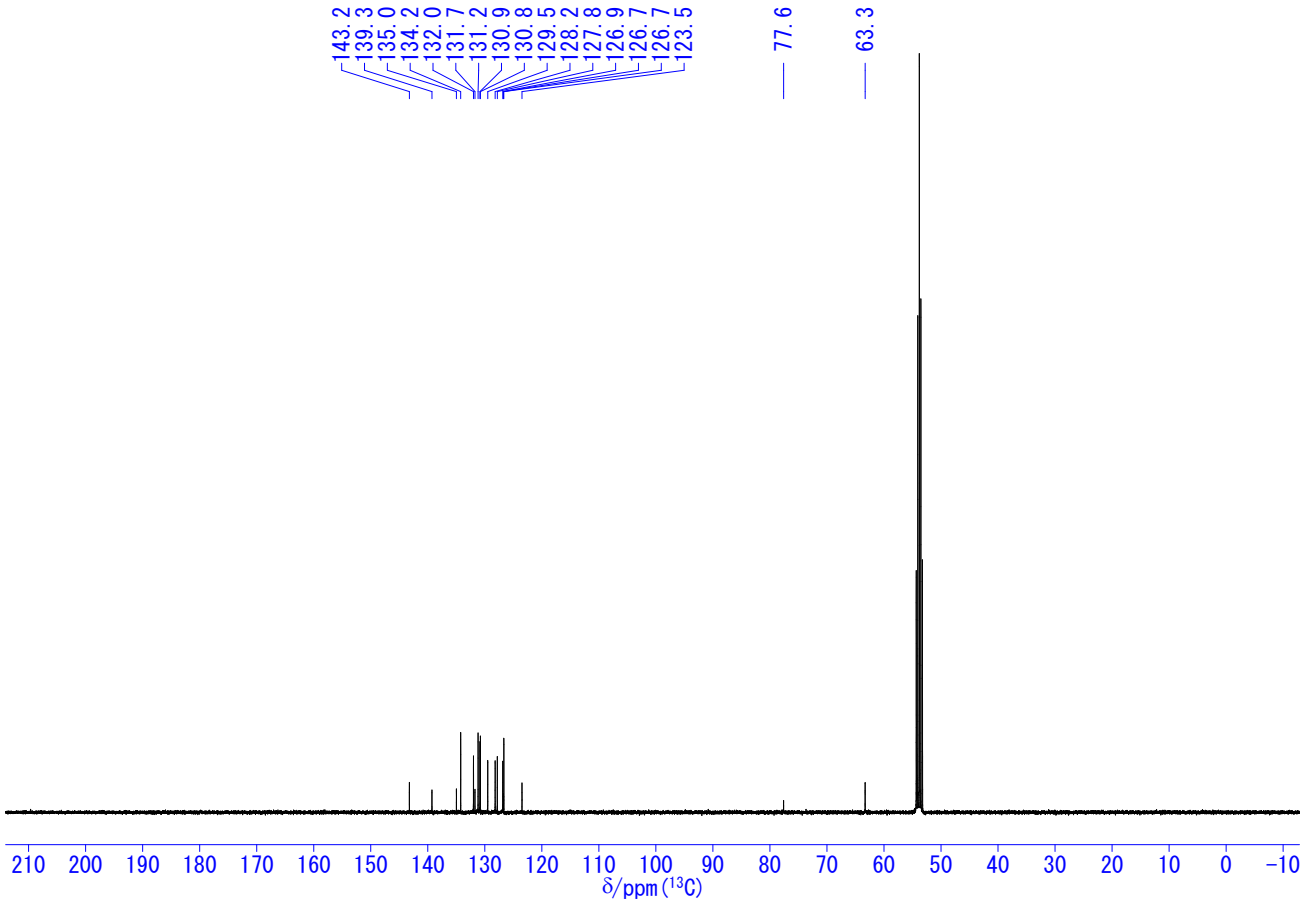

Chart S10. ^{13}C NMR spectrum of **C-3** in CD_2Cl_2.

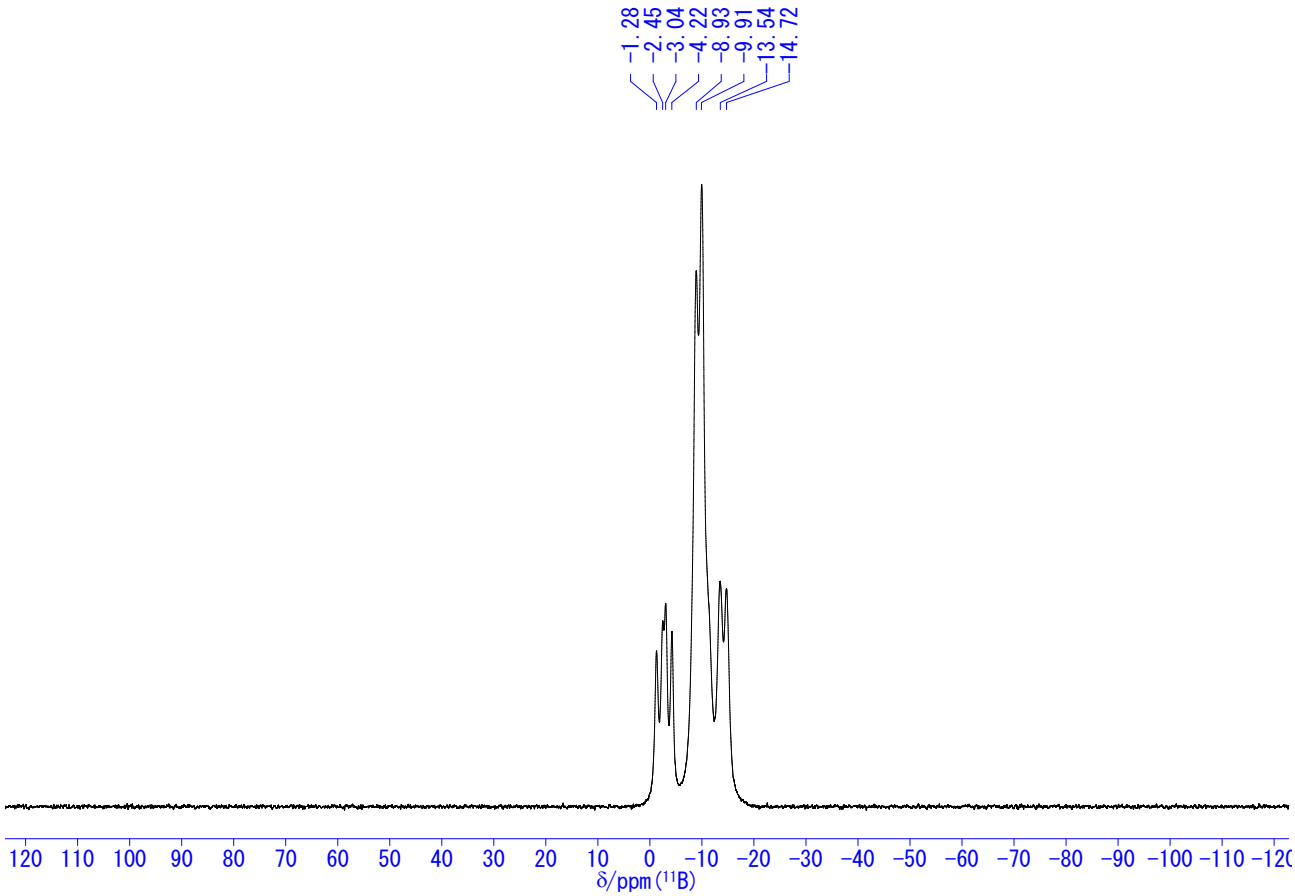

Chart S11. ^{11}B NMR spectrum of **C-3** in CD_2Cl_2.

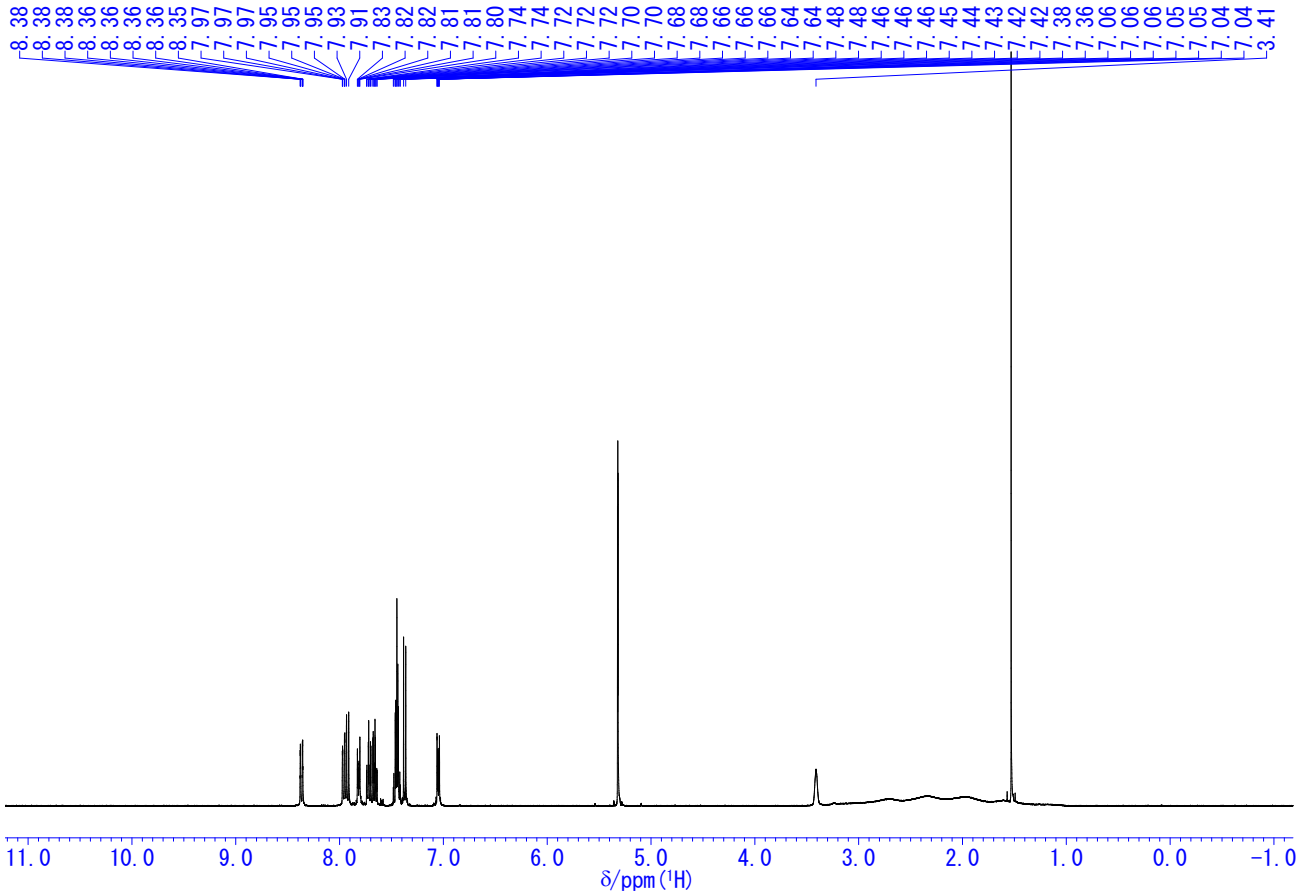

Chart S12. ^{1}H NMR spectrum of **B-3** in CD_2Cl_2.

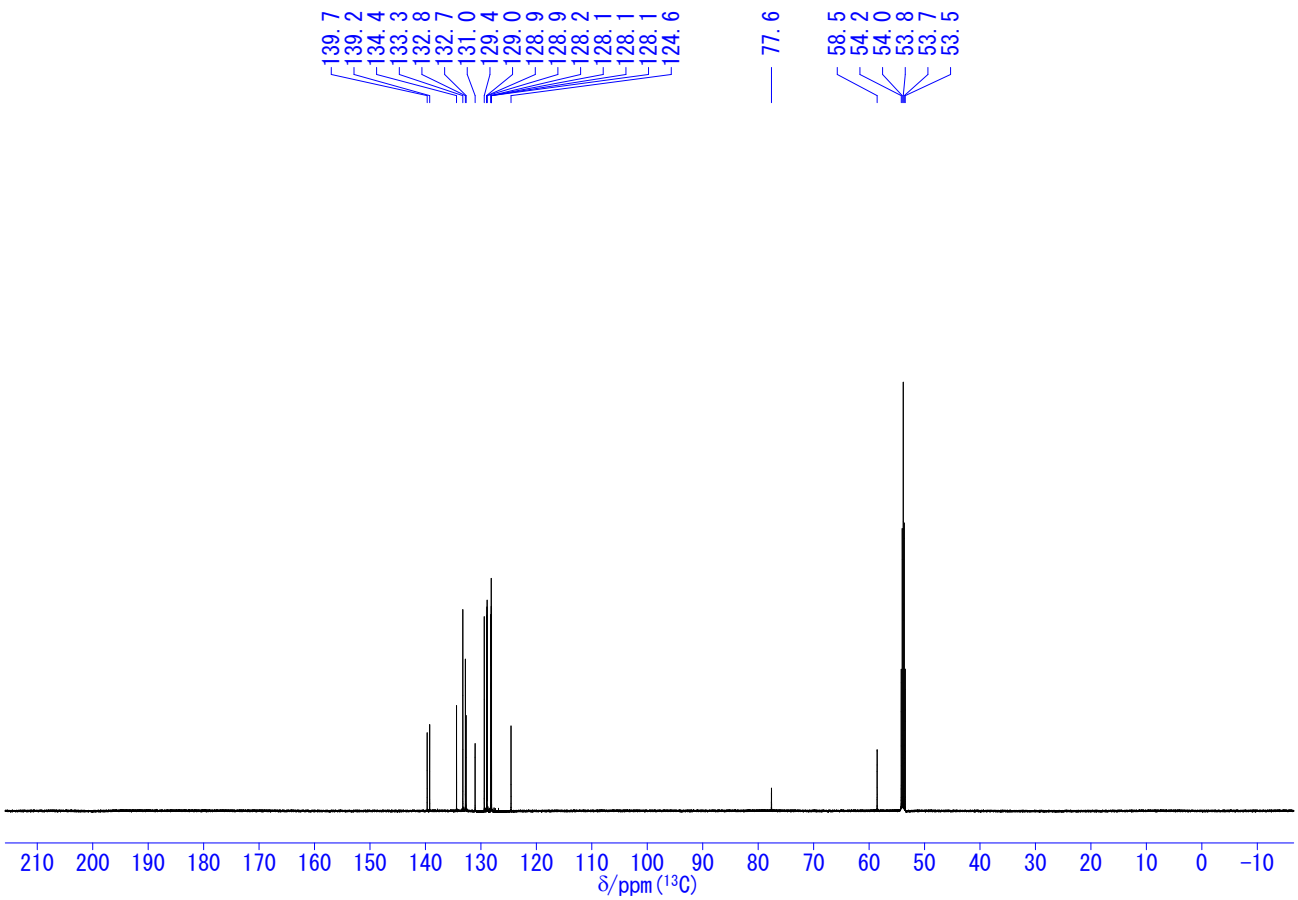

Chart S13. ^{13}C NMR spectrum of **B-3** in CD_2Cl_2.

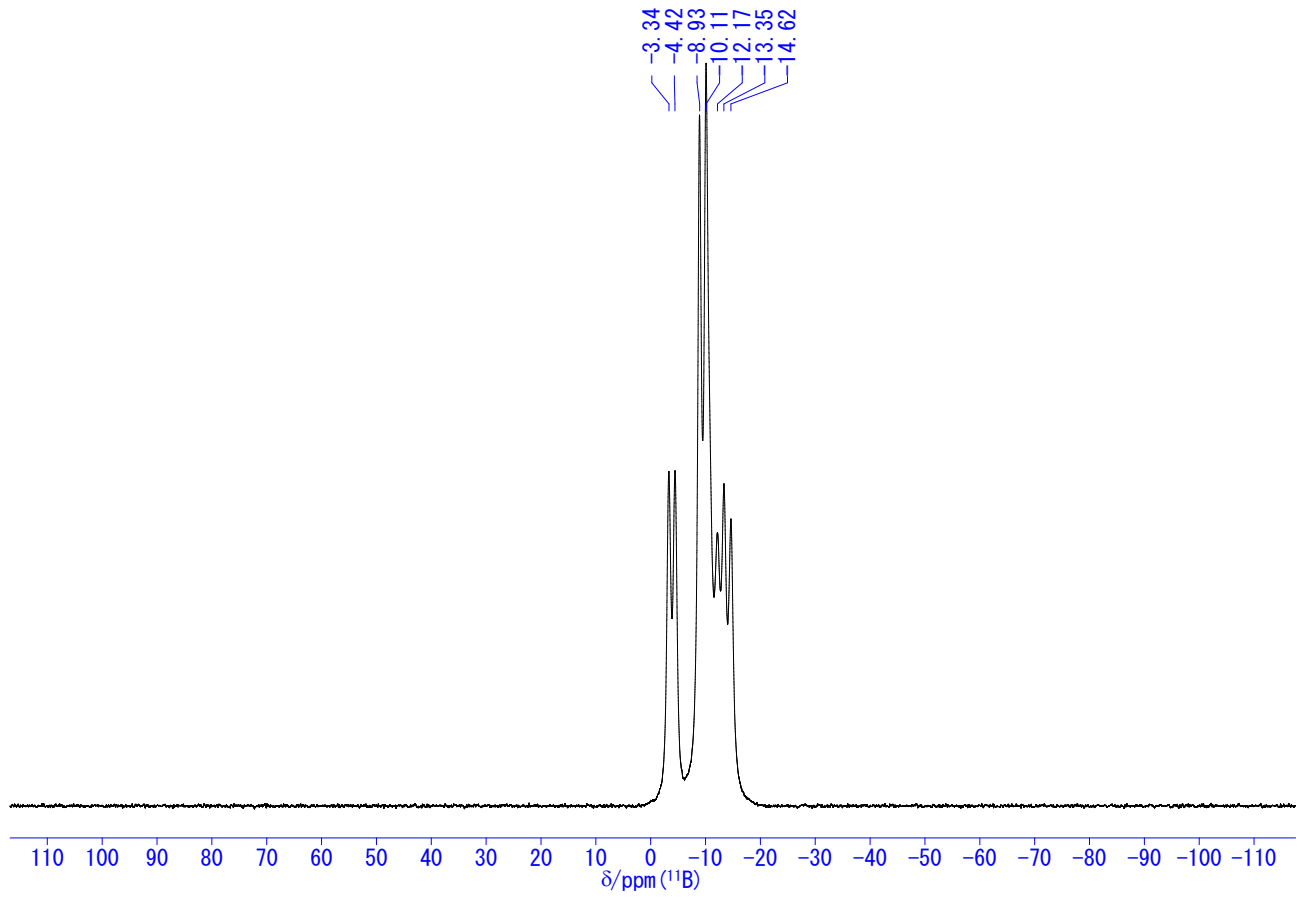

Chart S14. ^{11}B NMR spectrum of **B-3** in CD_2Cl_2.

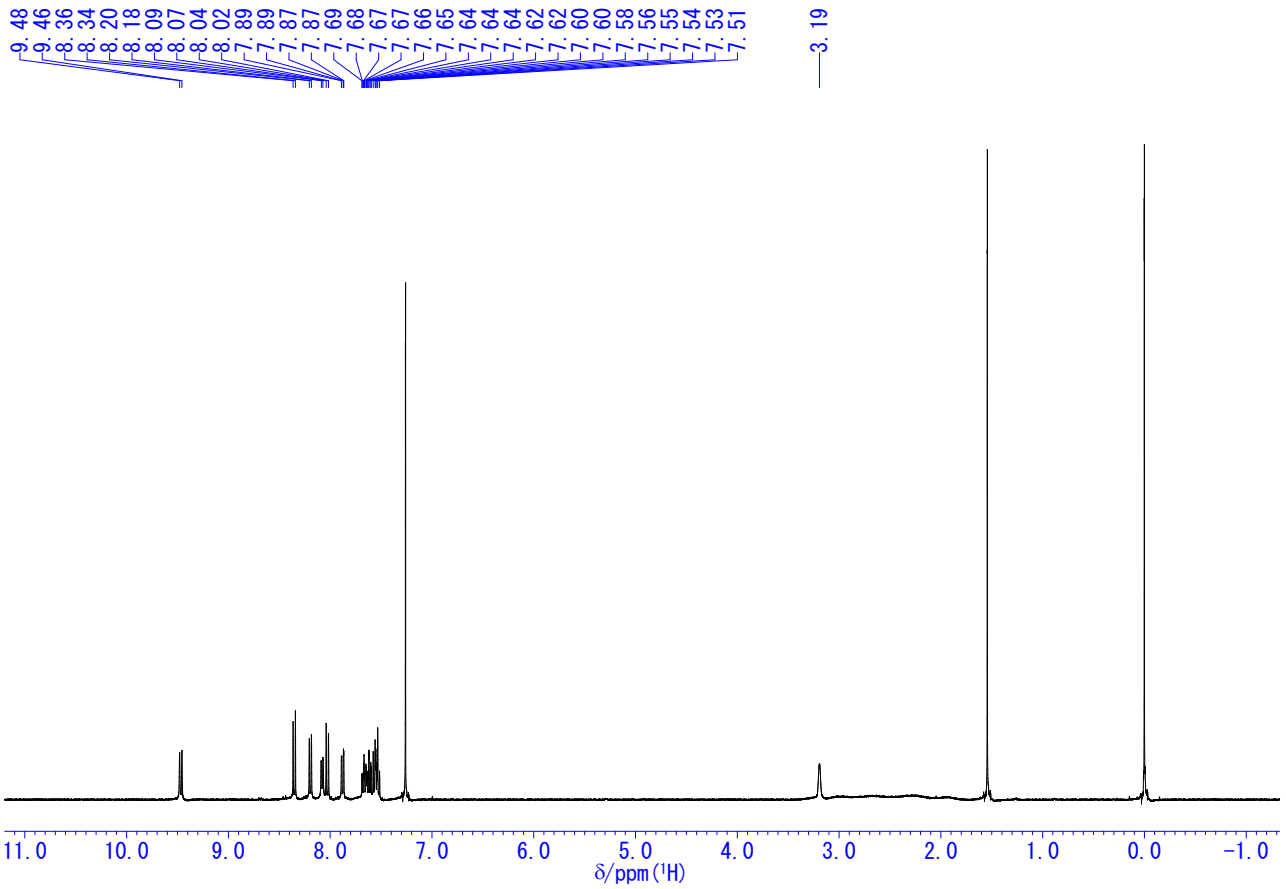

Chart S15. ^{1}H NMR spectrum of **CNaph** in $CDCl_3$.

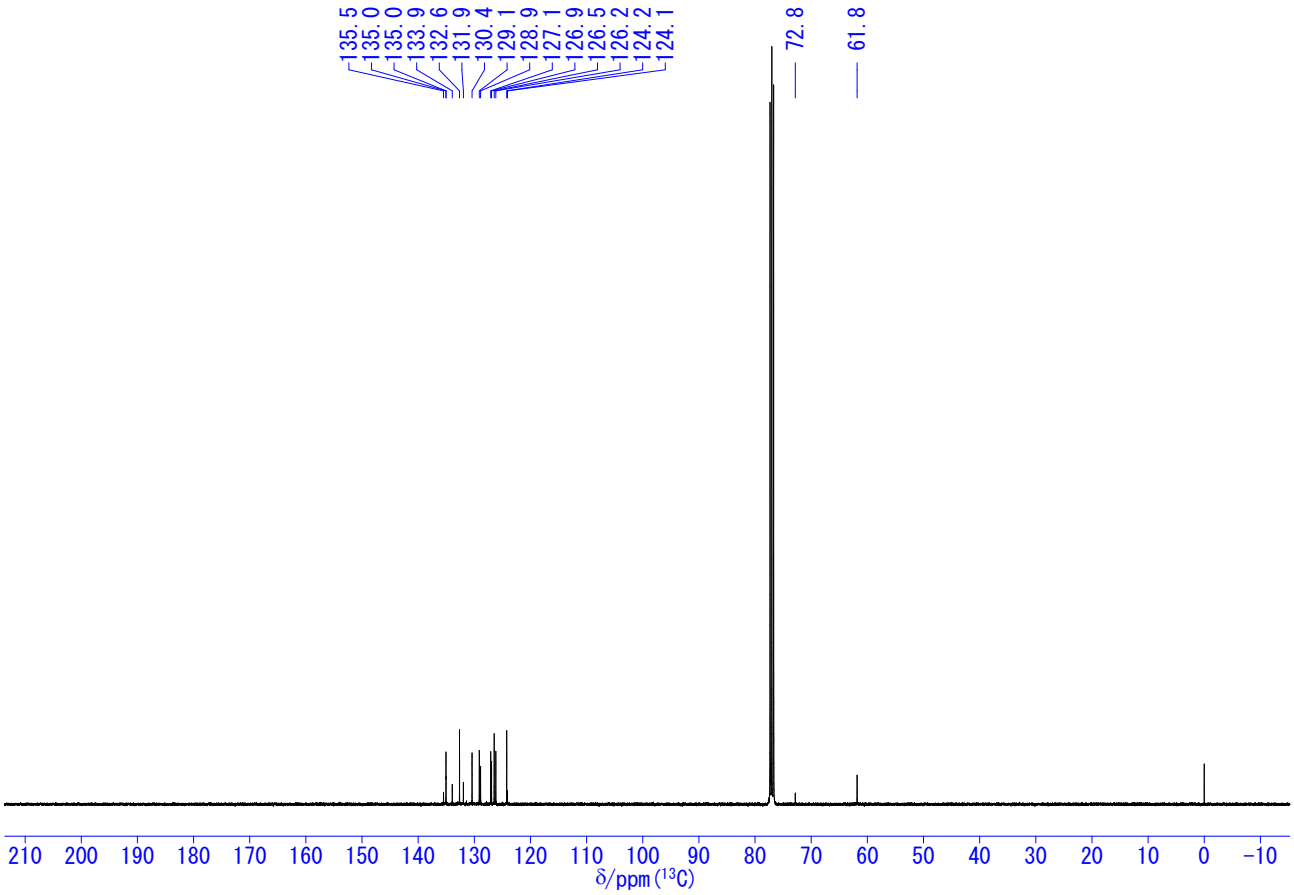

Chart S16. ^{13}C NMR spectrum of **CNaph** in $CDCl_3$.

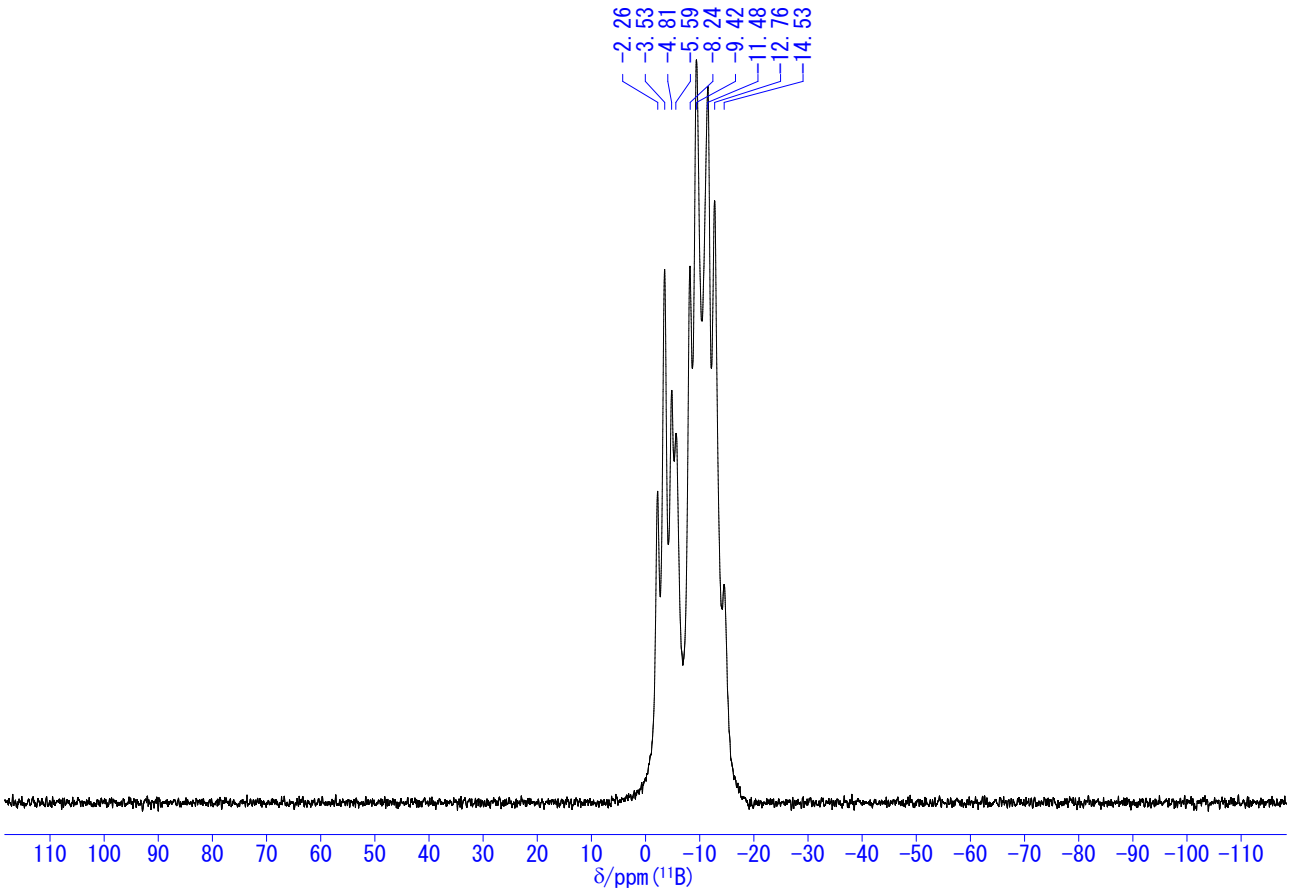

Chart S17. ^{11}B NMR spectrum of **CNaph** in $CDCl_3$.

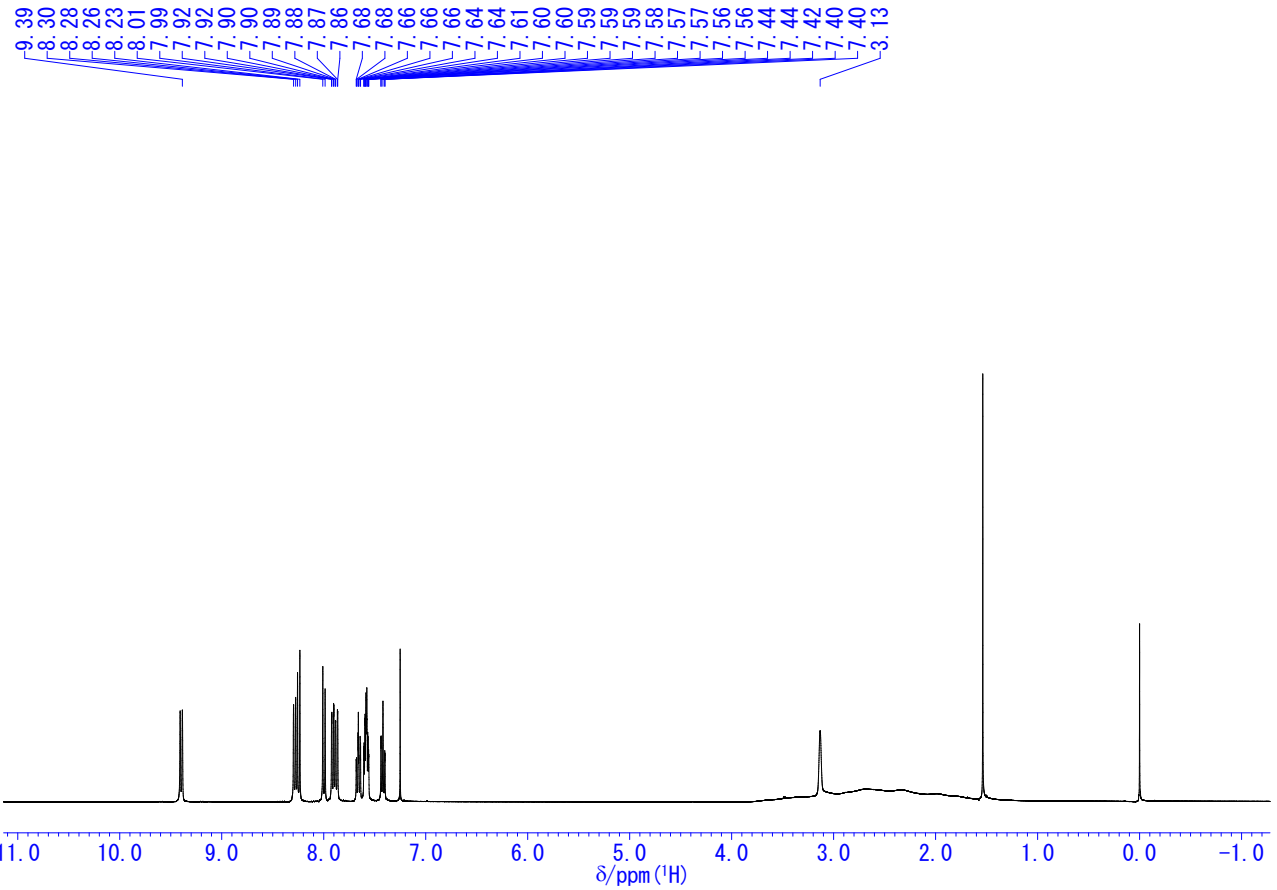

Chart S18. ^{1}H NMR spectrum of **BNaph** in $CDCl_3$.

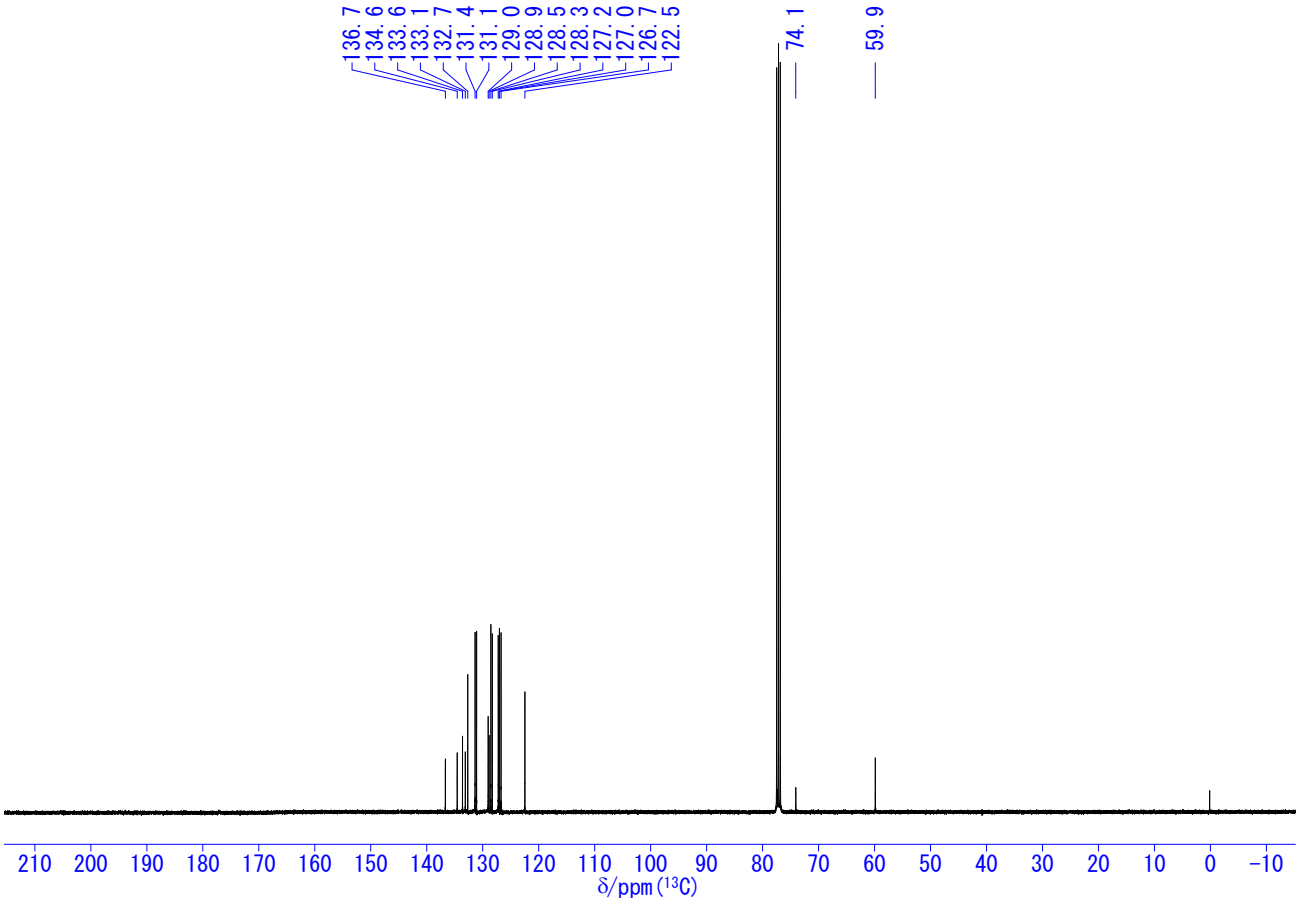

Chart S19. ^{13}C NMR spectrum of **BNaph** in $CDCl_3$.

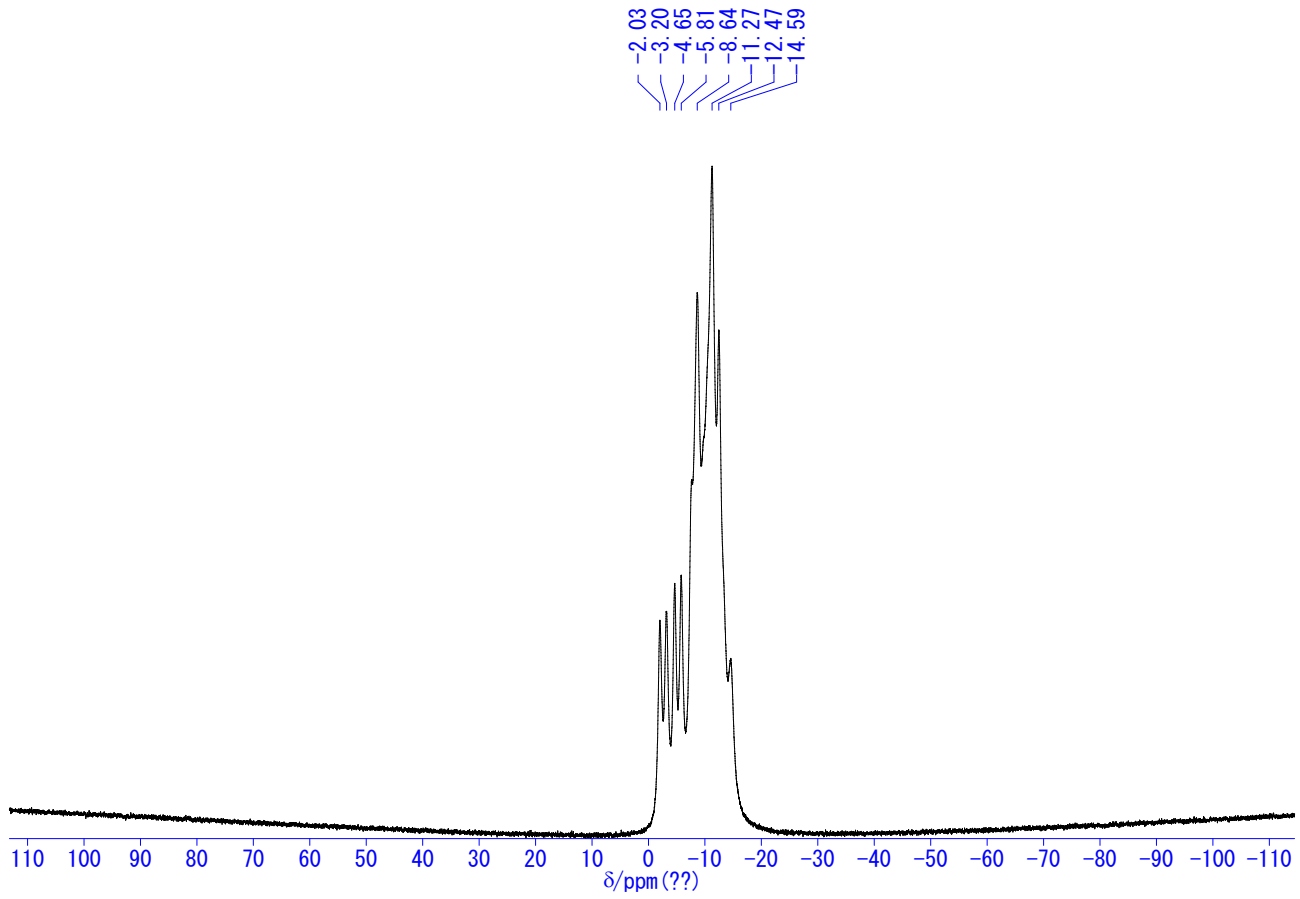

Chart S20. ^{11}B NMR spectrum of **BNaph** in $CDCl_3$.

Single Crystal X-ray Structures

X-ray crystallographic analyses were carried out by a Rigaku Saturn 724+ with MicroMax-007 HF CCD diffractometer with Varimax Mo optics using graphite-monochromated MoKα radiation. The structures were solved with SHELXT 2015[2] and refined on F^2 with SHELXL 2015[3] on Olex 2-1.2.[4] All hydrogen atoms were placed at calculated positions and refined using a riding model. The program Mercury 4.2.0[5] was used to generate the X-ray structural diagram.

Table S1. Selected crystallographic data of the synthesized compounds

	CNaph (CCDC: 2236202)	**BNaph** (CCDC: 2236203)
Empirical formula	$C_{18}H_{20}B_{10}$	$C_{18}H_{20}B_{10}$
Formula weight	344.44	344.44
Temperature (K)	143	143
Wavelength (Å)	0.71075	0.71075
Crystal system, space group	Triclinic, $P\bar{1}$	Monoclinic, $P2_1/n$
Unit cell dimensions	a = 10.227(5)	a = 10.943(3)
	b = 13.290(8)	b = 11.516(3)
	c = 14.005(7)	c = 14.661(4)
	α = 105.691(10)	α = 90
	β = 95.959(8)	β = 90.013(5)
	γ = 90.075(9)	γ = 90
V (Å^3)	1821.8(17)	1847.5(9)
Z, calculated density (Mg m^{-3})	4, 1.256	4, 1.238
Absorption coefficient	0.063	0.062
F(000)	712	712
Crystal size (mm)	0.04 × 0.04 × 0.02	0.09 × 0.06 × 0.02
θ range for data collection	3.024 –27.520	3.294–27.489
Limiting indices	–13≤h≤13, –17≤k≤16, -18≤l≤16	–13≤h≤12, –11≤k≤14, –19≤l≤19
Reflections collected (unique)	8014/3799 [R(int) = 0.0757]	15060/3311 [R(int) = 0.0641]
Goodness-of-fit on F^2	1.093	1.080
Final R indices [$I > 2\sigma(I)$]	R_1 = 0.1185, wR_2 = 0.2384	R_1 = 0.0646, wR_2 = 0.1318
R indices (all data)	R_1 = 0.2120, wR_2 = 0.2859	R_1 = 0.0835, wR_2 = 0.1435

Optical data

UV–vis absorption spectra were obtained on a SHIMADZU UV3600i Plus spectrophotometer. Photoluminescence (PL) spectra were measured with a HORIBA JOBIN YVON Fluorolog-3 spectrofluorometer. Because the second order signal of the LE band was overlapped to the ICT band, the LE and ICT regions were measured separately and merged afterwards. In addition, the ICT emission signals were weakened due to the sharp cut filter. Thus, the ICT signals should have been corrected by applying appropriate coefficients to connect with the LE signals smoothly. The PL lifetime measurement was performed on a Horiba FluoroCube spectrofluorometer system; excitation was carried out using a UV diode laser (NanoLED 292 nm). Temperature control in PL spectra and PL lifetime measurement was conducted by Oxford Optistat DN2. Fluorescence quantum yield (QY) was recorded on a HAMAMATSU Quantaurus-QY Plus C13534-01 model.

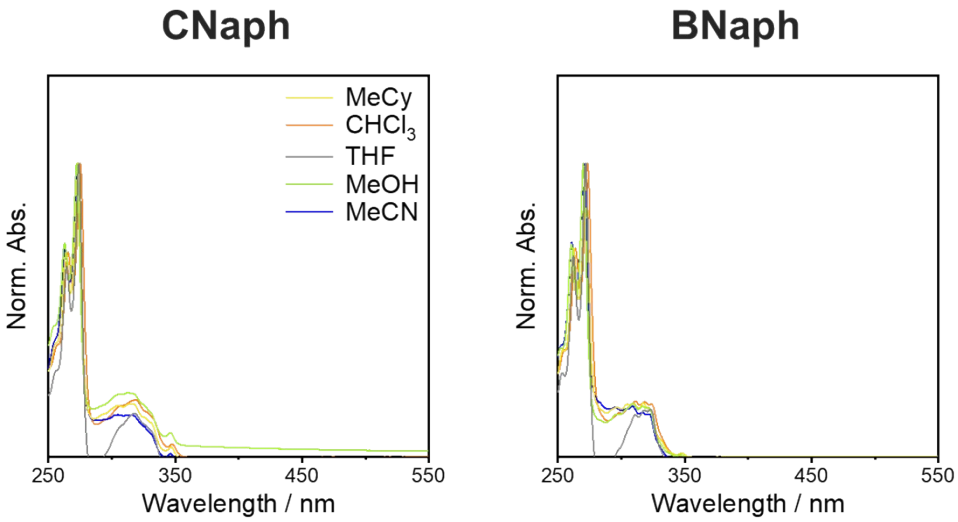

Figure S1. Absorption (abs.) spectra of **CNaph** (left) and **BNaph** (right) in various solvents.

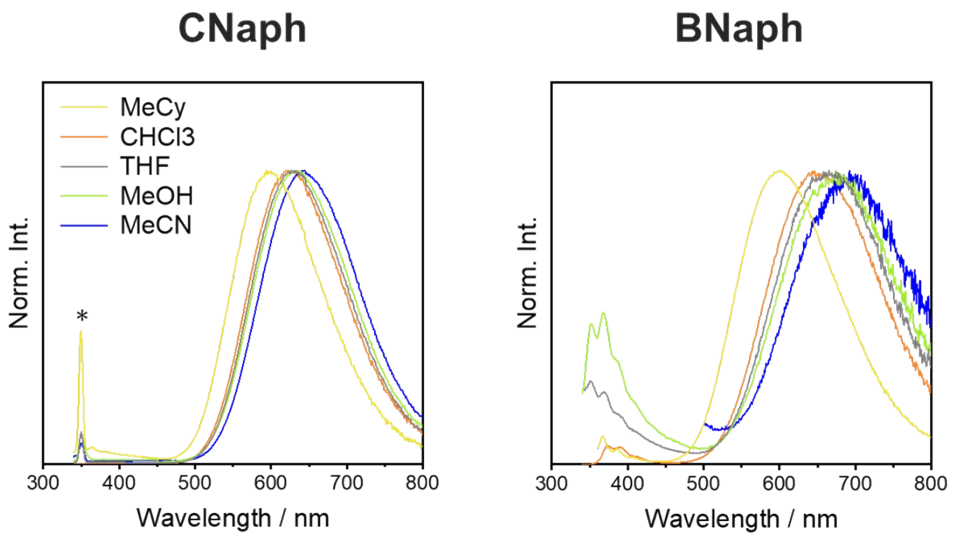

Figure S2. PL spectra of **CNaph** (left) and **BNaph** (right) in various solvents. An asterisk represents the scattering peak. The spectrum (< 500 nm) of **BNaph** in MeCN were omitted due to the noisy pattern.

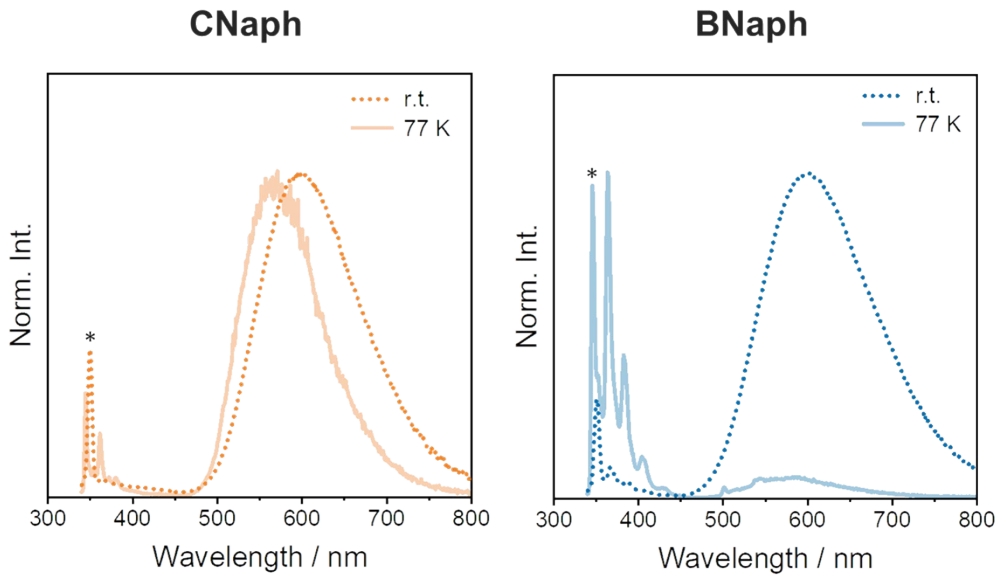

Figure S3. PL spectra of **CNaph** (left) and **BNaph** (right) in methylcyclohexane at r.t. (fluid state) and 77 K (glass matrix). An asterisk represents the scattering peak.

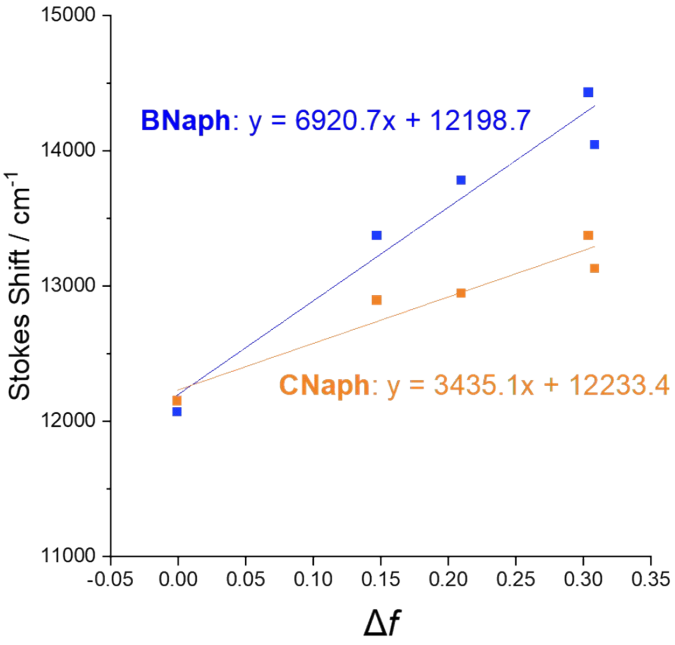

Figure S4. Lippert-Mataga plot of **CNaph** (orange) and **BNaph** (blue) in various solvents.

The differences in the dipole moments ($\Delta\mu$) between the ground and excited states was estimated as follows:

$$(slope) = \frac{1}{4\pi\varepsilon_0}\frac{2(\Delta\mu)^2}{hca^3}$$

where ε_0 is electreic constant, h is Planck constant, c is velocity of light, and a is onsager cavity radus. In this research, a was estimated by DFT calculation as described later.

Computational methods

All calculations were performed using Gaussian 16 C01 package[6] at CAM-B3LYP/6-31+G(d,p) level of theory.

One isolated molecule

The potential energy curve and optimized structure were calculated by the density functional theory (DFT) for S_0 states and time dependent-DFT (TD-DFT) for S_1 states. Because S_1 structural optimization of **BNaph** from pristine S_0 optimized structure was trapped by local minimum structure, C_{cage}–C_{cage} bond of S_0 optimized structure was elongated to 2.0 Å and the structure was treated as an initial structure. The author performed the frequency calculation at the optimized structure to confirm that the structure was at the local minimum because no imaginary frequencies were found. The molecular radius was estimated by using the keyword "volume" for the optimized structure. Kohn-Sham orbitals (HOMO and LUMO) and natural transition orbitals (NTOs) were generated from the optimized structure using GaussView 6 (isovalue: 0.02).

QM/MM analyses

The molecular coordination for QM/MM analyses was extracted from single-crystal structures. The central one molecule was treated by TD-DFT method at CAM-B3LYP/6-31+G(d,p) level of theory. The surrounding molecules were arranged to cover the central molecule completely and fixed in optimizing the structure of the central molecule.

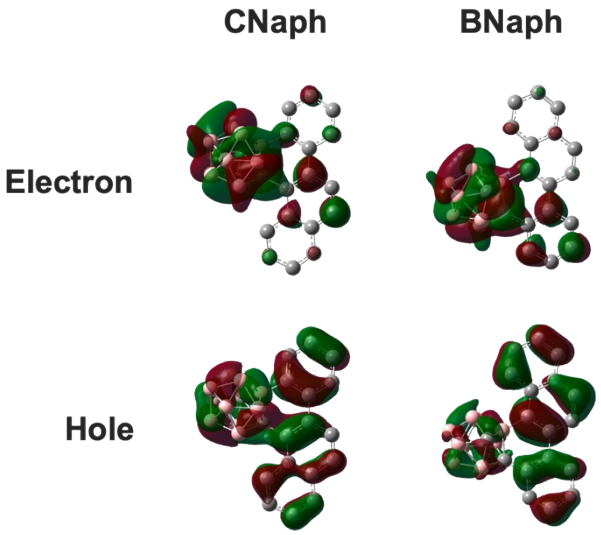

Figure S5. NTOs or **CNaph** and **BNaph** at S_1-optimized structures.

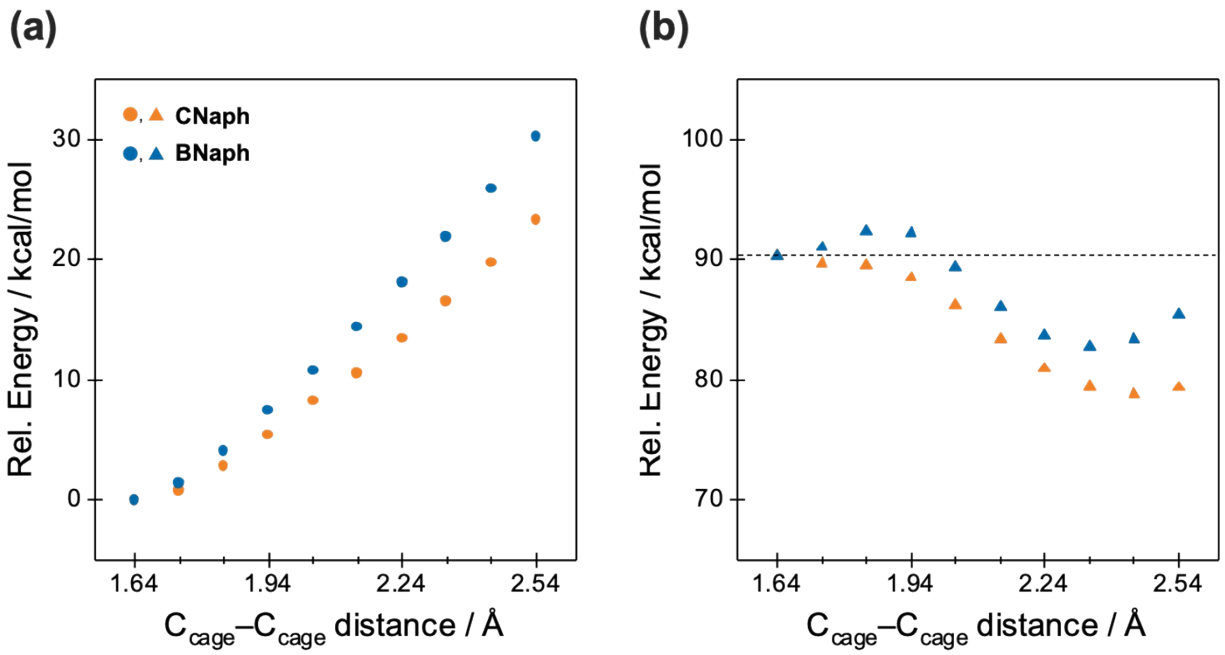

Figure S6. Enlarged energy levels at the (a) S_0 and (b) S_1 states of **CNaph** (orange) and **BNaph** (blue).

Table S2. Benchmark TD-DFT calculation for an isolated molecule.

Compound	geometry	condition[a]	transition energy (eV)	wavelength (nm)	*f*	transition type
CNaph	S_0	B3LYP	3.7713	328.76	0.1274	LE
		PBE0-D3	3.8933	318.45	0.1283	LE
		CAM-B3LYP	4.2214	293.70	0.1660	LE
		M06-2X	4.2463	291.98	0.1746	LE
	S_1	B3LYP	1.8664	664.29	0.0523	CT
		PBE0-D3	1.9888	623.41	0.0567	CT
		CAM-B3LYP	2.1105	587.46	0.0590	CT
		M06-2X	3.5680	347.49	0.2205	LE[b]
BNaph	S_0	B3LYP	3.7213	333.17	0.0862	LE
		PBE0-D3	3.8536	321.74	0.0964	LE
		CAM-B3LYP	4.2008	295.14	0.1231	LE
		M06-2X	4.2142	294.20	0.1195	LE
	S_1	B3LYP	1.6265	762.26	0.0190	CT
		PBE0-D3	1.7862	694.12	0.0224	CT
		CAM-B3LYP	2.2092	561.21	0.0285	CT
		M06-2X	3.6399	340.62	0.2198	LE[b]

[a] 6-31G+(d,p) basis set was used in all conditions.

[b] trapped by the local minimum when using the standard initial structures (as mentioned above).

Table S3. Optimized geometry of **CNaph** in the S_0 state

Center Number	Atomic Number	Coordinates (Angstroms)		
		x	y	z
1	6	0.355136	1.631741	0.03696
2	6	3.167656	1.244737	0.102437
3	6	0.860891	0.325616	-0.020939
4	6	-0.100196	-0.855556	0.035723
5	6	-2.111154	1.077445	0.144511
6	6	-1.140592	-1.132637	-1.21861
7	1	-1.029067	-0.454339	-2.054373
8	6	-1.460739	3.352062	-0.281585
9	1	-0.717308	4.103964	-0.509098
10	6	2.301456	0.119951	-0.039809
11	6	-3.44746	1.488505	0.166295
12	1	-4.223972	0.746582	0.322818
13	6	2.959042	-1.132802	-0.211106
14	1	2.395851	-2.034452	-0.349353
15	6	-2.790073	3.745643	-0.275862
16	1	-3.039659	4.783394	-0.472585
17	6	-1.087885	2.018683	-0.033957
18	6	4.577091	1.095782	0.09991
19	1	5.184217	1.987735	0.222453
20	6	1.268716	2.710997	0.212181
21	1	0.881647	3.70796	0.359301
22	6	2.612063	2.53202	0.25804
23	1	3.273805	3.378304	0.415565
24	6	-3.795386	2.81664	-0.024398
25	1	-4.836666	3.121123	-0.003577
26	6	4.325801	-1.252699	-0.223964
27	1	4.764399	-2.235236	-0.365291
28	6	5.159357	-0.130432	-0.058877
29	1	6.238658	-0.239305	-0.06396
30	5	-1.523567	-2.765949	-1.438668
31	1	-1.679437	-3.145794	-2.547206
32	5	0.241137	-2.366464	0.783322
33	1	1.285789	-2.530498	1.298516
34	5	-1.295742	-2.970546	1.401282
35	1	-1.317977	-3.637393	2.380475
36	5	-2.668339	-1.638878	-0.71361
37	1	-3.602987	-1.256319	-1.327983
38	5	-2.389984	-3.213373	0.032093
39	1	-3.221903	-4.056588	0.010645
40	5	-0.905723	-1.251683	1.511464
41	1	-0.604561	-0.619555	2.46304
42	5	0.099353	-2.242763	-0.990283
43	1	0.977734	-2.241245	-1.772144
44	5	-0.650665	-3.583923	-0.139444
45	1	-0.223414	-4.68033	-0.27545
46	5	-1.75952	-0.42709	0.211414
47	5	-2.53901	-1.758499	1.046002
48	1	-3.467179	-1.53635	1.748647

Table S4. Optimized geometry of **CNaph** in the S_1 state

Center Number	Atomic Number	Coordinates (Angstroms)		
		x	y	z
1	6	0.5889176	1.6341075	0.0941202
2	6	3.3515678	0.9553065	0.0077386
3	6	0.968599	0.2540181	0.084104
4	6	-0.0687522	-0.7713871	0.2232078
5	6	-1.8759178	1.1997348	-0.2270328
6	6	-1.6591085	-1.3269266	-1.5324267
7	1	-1.6379145	-0.889702	-2.5220654
8	6	-1.1126098	3.4537442	0.3149772
9	1	-0.3550441	4.1416549	0.6628745
10	6	2.3704457	-0.079685	-0.0104764
11	6	-3.1522355	1.7426524	-0.4812377
12	1	-3.9560688	1.0686806	-0.7528994
13	6	2.8496681	-1.4092567	-0.163728
14	1	2.1569174	-2.2281569	-0.2345084
15	6	-2.3812981	3.9394312	0.1140171
16	1	-2.5899805	4.9886734	0.2956373
17	6	-0.7986396	2.0879289	0.0900974
18	6	4.721458	0.64297	-0.0727249
19	1	5.4407956	1.4559717	-0.0505817
20	6	1.614371	2.6262432	0.0840791
21	1	1.3424696	3.6708951	0.0587858
22	6	2.9334425	2.3115348	0.0673448
23	1	3.6851392	3.0945408	0.0607699
24	6	-3.4108586	3.083544	-0.3245169
25	1	-4.4085885	3.4746917	-0.4943357
26	6	4.1944329	-1.6908689	-0.2506793
27	1	4.51462	-2.7203373	-0.3699961
28	6	5.14571	-0.6617146	-0.1919695
29	1	6.2044916	-0.8905431	-0.2544505
30	5	-2.021911	-2.861225	-1.2560973
31	1	-2.2438914	-3.5735101	-2.1766096
32	5	-0.0056979	-2.256363	0.8981386
33	1	1.0042948	-2.6144855	1.3943242
34	5	-1.6109096	-2.5673646	1.6173613
35	1	-1.6904929	-3.0651677	2.6919694
36	5	-3.0264017	-1.5193801	-0.6621357
37	1	-4.0435656	-1.1556853	-1.151393
38	5	-2.7616696	-2.9564424	0.3460177
39	1	-3.6416338	-3.7252922	0.5508416
40	5	-1.0220725	-0.9105881	1.517229
41	1	-0.8154869	-0.1772473	2.4241625
42	5	-0.3145699	-2.0996683	-0.9232655
43	1	0.5742893	-2.3115293	-1.6774702
44	5	-1.0590015	-3.4249053	0.1430814
45	1	-0.704053	-4.556586	0.1611685
46	5	-1.6546744	-0.331516	-0.1760598
47	5	-2.7131245	-1.2981851	1.0408786
48	1	-3.5612894	-0.8069359	1.7086716

Table S5. Optimized geometry of **BNaph** in the S_0 state

Center Number	Atomic Number	Coordinates (Angstroms)		
		x	y	z
1	6	-2.4082166	-0.0472114	-0.0965381
2	6	-3.3732242	0.9774219	0.1129447
3	6	1.72665	-0.3176378	-0.0333943
4	6	-1.0002319	0.2716655	-0.0918185
5	6	3.2227997	1.6615437	-0.0662971
6	1	4.0511949	0.9654641	-0.0440905
7	6	3.4801186	3.0190028	-0.1496039
8	1	4.5026362	3.3789501	-0.1828728
9	6	-2.9232953	2.2990099	0.338031
10	1	-3.6527522	3.0774127	0.5420963
11	6	1.0714323	-1.0437891	1.269081
12	1	0.8054438	-0.3791606	2.0806406
13	6	1.916326	1.1674151	-0.0233726
14	6	-4.7574072	0.6749573	0.1108706
15	1	-5.4637274	1.4829437	0.2785401
16	6	-2.9082468	-1.3609808	-0.3146777
17	1	-2.2215206	-2.1712642	-0.4975112
18	6	-0.6059788	1.601024	0.0547017
19	6	0.8172137	2.0481419	-0.0331227
20	6	-4.2534189	-1.6298314	-0.3210826
21	1	-4.5932143	-2.6451409	-0.4986594
22	6	-1.5964961	2.5970002	0.3041344
23	1	-1.3025145	3.6171093	0.5055078
24	6	1.1117978	3.4180164	-0.1536154
25	1	0.3086798	4.1363984	-0.2324541
26	6	2.4082351	3.9009392	-0.2103748
27	1	2.5773828	4.9683659	-0.3074195
28	5	1.2700387	-1.131826	-1.4615053
29	1	1.1487764	-0.4785018	-2.4385262
30	5	0.2364496	-2.4509093	-0.9172002
31	1	-0.6341372	-2.8654393	-1.6021924
32	5	1.2051995	-3.5122161	0.131108
33	1	0.9946158	-4.6755655	0.2072037
34	6	-5.1966731	-0.6040956	-0.102243
35	1	-6.2581268	-0.8294361	-0.1065948
36	5	2.7326707	-1.263433	1.0089985
37	1	3.4819854	-0.6803765	1.7077303
38	5	0.0940113	-2.3406544	0.8487426
39	1	-0.8644036	-2.5505261	1.5060626
40	5	1.6995164	-2.587022	1.5501716
41	1	1.8001675	-2.9415557	2.6733404
42	5	1.9423279	-2.7578333	-1.2920406
43	1	2.2702841	-3.3682052	-2.25309
44	5	2.8723638	-1.3629306	-0.7507983
45	1	3.8148067	-0.8844126	-1.276194
46	5	0.0982049	-0.8550543	-0.1512678
47	5	2.8528658	-2.8310771	0.2336284
48	1	3.8278763	-3.4878296	0.377562

Table S6. Optimized geometry of **BNaph** in the S_1(LE) state

Center Number	Atomic Number	Coordinates (Angstroms)		
		x	y	z
1	6	-2.3950299	-0.0464904	-0.0844882
2	6	-3.3715927	0.9940765	0.094721
3	6	1.7169489	-0.3254209	-0.0603225
4	6	-1.00959	0.2454505	-0.061373
5	6	3.2232957	1.641233	-0.0760362
6	1	4.0456496	0.9369191	-0.061672
7	6	3.503959	2.9965356	-0.1325546
8	1	4.5313886	3.3416127	-0.1588574
9	6	-2.903861	2.3248958	0.328808
10	1	-3.6320127	3.1062769	0.5252141
11	6	1.1026319	-1.0551951	1.281852
12	1	0.8666752	-0.3816432	2.0952673
13	6	1.9169274	1.1539162	-0.0536162
14	6	-4.7315	0.7096831	0.0775546
15	1	-5.4357615	1.5229598	0.2286809
16	6	-2.9199517	-1.3586995	-0.2684246
17	1	-2.2446225	-2.1861947	-0.4154851
18	6	-0.5703912	1.6558308	0.0583122
19	6	0.8042977	2.0623829	-0.0474793
20	6	-4.2915138	-1.6203157	-0.2894829
21	1	-4.6274155	-2.6407166	-0.4420869
22	6	-1.56956	2.6254586	0.3094773
23	1	-1.2854922	3.6481133	0.5164221
24	6	1.1395173	3.4485282	-0.1509596
25	1	0.3485811	4.1799068	-0.2422532
26	6	2.4350166	3.9028855	-0.1868627
27	1	2.6250313	4.9678129	-0.2744832
28	5	1.2130914	-1.150072	-1.4618956
29	1	1.0571407	-0.5060744	-2.4397999
30	5	0.1947181	-2.4666499	-0.8760216
31	1	-0.6990023	-2.8780507	-1.5339966
32	5	1.1936256	-3.5255725	0.1435935
33	1	0.9831695	-4.688398	0.2303326
34	6	-5.2116266	-0.5992004	-0.1203805
35	1	-6.2775631	-0.7964568	-0.1342067
36	5	2.7500429	-1.2727989	0.9601516
37	1	3.5267757	-0.6972033	1.6338845
38	5	0.1061224	-2.3470288	0.8905597
39	1	-0.8392707	-2.5502483	1.5710769
40	5	1.7332012	-2.5953042	1.5445389
41	1	1.8743207	-2.9519806	2.6628848
42	5	1.8859016	-2.7787446	-1.3067159
43	1	2.1792913	-3.3971991	-2.2739723
44	5	2.8372405	-1.381524	-0.8014524
45	1	3.7656618	-0.9096743	-1.3571129
46	5	0.0850491	-0.8650883	-0.1122013
47	5	2.8428857	-2.8466923	0.1898832
48	1	3.8201962	-3.5057121	0.3054946

Table S7. Optimized geometry of **BNaph** in the S_1(ICT) state

Center Number	Atomic Number	Coordinates (Angstroms)		
		x	y	z
1	6	-2.3382445	0.0382751	0.0913521
2	6	-3.2662035	1.1022885	-0.1156649
3	6	1.7300165	-0.2595216	-0.3021192
4	6	-0.9153974	0.2778844	0.0722475
5	6	3.300586	1.6425262	-0.0884995
6	1	4.1152669	0.9460516	-0.2433563
7	6	3.5684775	2.9742205	0.1676704
8	1	4.5969712	3.3181617	0.2085527
9	6	-2.7716467	2.4105325	-0.3768937
10	1	-3.4795741	3.2050117	-0.5933896
11	6	0.9307652	-1.4865643	1.5322539
12	1	0.7058799	-1.072374	2.5062847
13	6	1.9856407	1.1565586	-0.13024
14	6	-4.6464825	0.8658494	-0.1092914
15	1	-5.3214771	1.6993724	-0.2783343
16	6	-2.8917544	-1.2507904	0.2773485
17	1	-2.2383544	-2.0921806	0.4181119
18	6	-0.4826683	1.6495245	-0.0852075
19	6	0.9096957	2.0674972	0.04762
20	6	-4.2598246	-1.4671272	0.288269
21	1	-4.6350601	-2.4731973	0.4407266
22	6	-1.4368697	2.6646116	-0.3690491
23	1	-1.0951074	3.6619502	-0.6069017
24	6	1.2170086	3.4165914	0.3381434
25	1	0.4192768	4.1139219	0.5595878
26	6	2.5176979	3.8690779	0.4034938
27	1	2.7211923	4.9060765	0.6466267
28	5	1.0549413	-1.0317947	-1.543862
29	1	0.7590031	-0.3945904	-2.4994252
30	5	0.0346073	-2.3646925	-0.9440759
31	1	-0.9394012	-2.6085444	-1.5790075
32	5	1.0794003	-3.6097918	-0.1815119
33	1	0.8746281	-4.7743309	-0.2854329
34	6	-5.1481207	-0.4089581	0.0995514
35	1	-6.2191257	-0.5809512	0.1062833
36	5	2.472228	-1.3416113	0.8824671
37	1	3.3311037	-0.87367	1.5530636
38	5	0.0073053	-2.6054338	0.7981991
39	1	-0.945726	-2.9932006	1.3856351
40	5	1.6496666	-2.9293863	1.3486467
41	1	1.9331493	-3.5352198	2.3274868
42	5	1.6854749	-2.6837946	-1.5402431
43	1	1.9128022	-3.2023215	-2.5837336
44	5	2.7245171	-1.3619726	-0.9399977
45	1	3.7154868	-0.9667557	-1.4579885
46	5	0.205359	-0.8536386	0.1200776
47	5	2.702373	-2.8825921	-0.0769951
48	1	3.6936471	-3.5345244	-0.0842231

Table S8. Result of TD-DFT calculation for **CNaph** in the S_0 geometry

Excited State	Energy / eV	Wavelength / nm	*f*	Composition	Coefficient
1	4.2214	293.70	0.1660		
				HOMO–1 -> LUMO+1	–0.17046
				HOMO -> LUMO	0.67197
2	4.3134	287.44	0.0255		
				HOMO–3 -> LUMO	–0.12242
				HOMO–1 -> LUMO	0.53686
				HOMO -> LUMO+1	0.38262
3	4.8947	253.30	0.0843		
				HOMO–3 -> LUMO+2	0.13694
				HOMO–2 -> LUMO	0.46303
				HOMO–2 -> LUMO+1	0.17750
				HOMO–2 -> LUMO+11	0.10012
				HOMO–1 -> LUMO	0.16912
				HOMO–1 -> LUMO+2	0.18828
				HOMO -> LUMO+1	–0.20600
				HOMO -> LUMO+2	–0.26186

Table S9. Result of TD-DFT calculation for **CNaph** in the S_1 geometry

Excited State	Energy / eV	Wavelength / nm	*f*	Composition	Coefficient
1	2.1105	587.46	0.0590		
				HOMO–4 -> LUMO	–0.10932
				HOMO–2 -> LUMO	0.18859
				HOMO -> LUMO	–0.65304
2	3.0040	412.73	0.0880		
				HOMO–6 -> LUMO	0.13818
				HOMO–4 -> LUMO	0.24780
				HOMO–2 -> LUMO	–0.50292
				HOMO–1 -> LUMO	0.29142
				HOMO -> LUMO	–0.24564
3	3.2961	376.16	0.1396		
				HOMO–4 -> LUMO	–0.12064
				HOMO–2 -> LUMO	0.26993
				HOMO–1 -> LUMO	0.62111

Table S10. Result of TD-DFT calculation for **BNaph** in the S_0 geometry

Excited State	Energy / eV	Wavelength / nm	*f*	Composition	Coefficient
1	4.2008	295.14	0.1231		
				HOMO–1 -> LUMO	–0.10455
				HOMO–1 -> LUMO+1	0.17198
				HOMO -> LUMO	0.65467
2	4.3413	285.59	0.0458		
				HOMO–1 -> LUMO	0.49631
				HOMO -> LUMO	0.15840
				HOMO -> LUMO+1	–0.41343
3	4.9247	251.76	0.1122		
				HOMO–3 -> LUMO	–0.12682
				HOMO–3 -> LUMO+2	0.16187
				HOMO–2 -> LUMO	–0.31692
				HOMO–2 -> LUMO+1	–0.15139
				HOMO–1 -> LUMO	–0.11632
				HOMO–1 -> LUMO+1	0.14641
				HOMO–1 -> LUMO+2	0.22063
				HOMO -> LUMO+2	0.44839

Table S11. Result of TD-DFT calculation for **BNaph** in the S_1(LE) geometry

Excited State	Energy / eV	Wavelength / nm	*f*	Composition	Coefficient
1	3.6170	342.78	0.2227		
				HOMO–1 -> LUMO+1	0.12320
				HOMO -> LUMO	0.68853
2	4.0526	305.94	0.0255		
				HOMO–1 -> LUMO	0.51931
				HOMO -> LUMO+1	–0.41646
3	4.6587	266.14	0.6394		
				HOMO–3 -> LUMO	–0.15762
				HOMO–2 -> LUMO	–0.10305
				HOMO–1 -> LUMO	–0.37960
				HOMO -> LUMO+1	–0.46443
				HOMO -> LUMO+2	0.25774

Table S12. Result of TD-DFT calculation for **BNaph** in the S_1(ICT) geometry

Excited State	Energy / eV	Wavelength / nm	*f*	Composition	Coefficient
1	2.2092	561.21	0.0285		
				HOMO–2 -> LUMO	0.13135
				HOMO -> LUMO	0.67670
2	3.3897	365.76	0.0445		
				HOMO–2 -> LUMO	0.14682
				HOMO–1 -> LUMO	0.66040
				HOMO -> LUMO	–0.11110
3	3.4486	359.53	0.0246		
				HOMO–6 -> LUMO	0.15296
				HOMO–5 -> LUMO	–0.26122
				HOMO–4 -> LUMO	0.33279
				HOMO–3 -> LUMO	0.17892
				HOMO–2 -> LUMO	0.46081
				HOMO–1 -> LUMO	–0.12391
				HOMO -> LUMO	–0.13307

Table S13. Results of QM/MM calculation for the S_1–S_0 transitions of **CNaph**

Condition	Energy / eV	Wavelength / nm	*f*	Composition	Coefficient
isolated one molecule	2.1105	587.46	0.0590		
				HOMO–4 -> LUMO	–0.10932
				HOMO–2 -> LUMO	0.18859
				HOMO -> LUMO	–0.65304
QM/MM	2.5541	485.43	0.1078		
				HOMO–2 -> LUMO	–0.12656
				HOMO -> LUMO	–0.68011

Table S14. Results of QM/MM calculation for the S_1–S_0 transitions of **BNaph**

Condition	Energy / eV	Wavelength / nm	*f*	Composition	Coefficient
isolated one molecule	2.2092	561.21	0.0285		
				HOMO–2 -> LUMO	0.13135
				HOMO -> LUMO	0.67670
QM/MM	2.4592	504.16	0.0425		
				HOMO–2 -> LUMO	–0.12692
				HOMO -> LUMO	–0.67702

References

(1) L. J. P. van der Boon, L. van Gelderen, T. R. de Groot, M. Lutz, J. C. Slootweg, A. W. Ehlers and K. Lammertsma, *Inorg. Chem.*, **2018**, *57*, 12697–12708.

(2) Sheldrick, G. M. *Acta Crystallogr. Sect. A Found. Crystallogr.* **2015**, *71*, 3–8.

(3) Sheldrick, G. M. *Acta Crystallogr. Sect. C Struct. Chem.* **2015**, *71*, 3–8.

(4) Dolomanov, O. V.; Bourhis, L. J. Gildea, R. J.; Howard, J. A. K; Puschmanna, H. *J. Appl. Cryst.* **2009**, *42*, 339–341.

(5) C. F. Macrae, P. R. Edgington, P. McCabe, E. Pidcock, G. P. Shields, R. Taylor, M. Towler, J. van de Streek. *J. Appl. Cryst.* **2006**, *39*, 453–457.

(6) Gaussian 16, Revision C.01, M. J. Frisch, G. W. Trucks, H. B. Schlegel, G. E. Scuseria, M. A. Robb, J. R. Cheeseman, G. Scalmani, V. Barone, G. A. Petersson, H. Nakatsuji, X. Li, M. Caricato, A. V. Marenich, J. Bloino, B. G. Janesko, R. Gomperts, B. Mennucci, H. P. Hratchian, J. V. Ortiz, A. F. Izmaylov, J. L. Sonnenberg, D. Williams-Young, F. Ding, F. Lipparini, F. Egidi, J. Goings, B. Peng, A. Petrone, T. Henderson, D. Ranasinghe, V. G. Zakrzewski, J. Gao, N. Rega, G. Zheng, W. Liang, M. Hada, M. Ehara, K. Toyota, R. Fukuda, J. Hasegawa, M. Ishida, T. Nakajima, Y. Honda, O. Kitao, H. Nakai, T. Vreven, K. Throssell, J. A. Montgomery, Jr., J. E. Peralta, F. Ogliaro, M. J. Bearpark, J. J. Heyd, E. N. Brothers, K. N. Kudin, V. N. Staroverov, T. A. Keith, R. Kobayashi, J. Normand, K. Raghavachari, A. P. Rendell, J. C. Burant, S. S. Iyengar, J. Tomasi, M. Cossi, J. M. Millam, M. Klene, C. Adamo, R. Cammi, J. W. Ochterski, R. L. Martin, K. Morokuma, O. Farkas, J. B. Foresman, and D. J. Fox, Gaussian, Inc., Wallingford CT, 2019.